KAZAN FEDERAL UNIVERSITY

DOOGLAV A.V., MOTYGULLIN I.G, TAGIROV M.S.

ELECTRONIC PARAMAGNETIC RESONANCE

Laboratory practical work

KAZAN

2019

UDC 537.635, 537.611.43

Approved by educational-methodological commission of Institute of Physics of Kazan Fedearl University

Reviewer:

Prof. **Garifullin I.A.** Zavoisky Physical—Technical Institute of Kazan Scientific Center of the Russian Academy of Sciences

Dooglav A.V., Motygullin I.G, Tagirov M.S.

Electron paramagnetic resonance/ Dooglav A.V., Motygullin I.G, Tagirov M.S. − Kazan: Kazan University Publishing House, 2019. − 84 p.

ISBN

The methodical textbook for laboratory practical work for master students of the Institute of Physics gives the basics of EPR theory, structure and principles of operation of the standard EPR spectrometer, procedure of measurement and calculation of the EPR spectrum of the Mn^{2+} ions in CaF_2 crystal.

UDC 537.635, 537.611.43

ISBN

CONTENTS

PART 1

ELECTRON PARAMAGNETIC RESONANCE

Many substances in a magnetized state gain the ability to absorb energy of electromagnetic waves impinging on such substance. This absorption has a resonance character, i.e. it appears only under certain condition between the electromagnetic wave length and the intensity of the static magnetic field that magnetizes the sample of substance. The phenomena of this type are called a magnetic resonance and play a considerable role in modern physics, chemistry, biology and technics as very effective tool for research of structure of substances and as a basis for making the very important technical devices.

One of the versions of magnetic resonance absorption – electron paramagnetic resonance appears as a result of interaction of the magnetic moments of electron shell of atoms of paramagnetic substances with the external (static $\mathbf{H}_o$ and high-frequency $\mathbf{H}_v$) magnetic fields. The essence of this physical effect is easy to understand if we recall the basic data on the magnetic properties of atoms and their interactions both with the external magnetic fields, and with each other.

1. Magnetic properties of atom

The atomic magnetism is generated by three origins:

a) orbital motion of electrons creating an orbital magnetic moment μ_l of each of them;
b) spin properties of an electron – existence with it an intrinsic mechanical $\mathbf{P}_s$ and magnetic μ_s moments;
c) the same properties of many nuclei possessing intrinsic mechanical $\mathbf{P}_I$ and magnetic μ_I moments.

The circulation of each electron around a nucleus with period T represents the analogue of a circular current with intensity $i=e/T$ (in SGS system), creating the orbital magnetic moment which value is equal to:

$$\mu_l = i \cdot S/c = \gamma_l \cdot P_l \qquad (1)$$

where S –area of contour run around by the electron; $P_l = \mathrm{h} \cdot \sqrt{l(l+1)}$ – mechanical moment of the electron orbital motions, l – orbital quantum number, and

$$\gamma_l = \mu_l/P_l = e / (2m_0c) \qquad (2)$$

– the so-called gyromagnetic ratio of orbital motion of an electron (strictly speaking, the gyromagnetic ratio is a quantity inverse to γ_l, however the used term was stated and does not cause misunderstanding).

Adding vectorially the orbital magnetic moments of all electrons of atom, they form the resulting magnetic moment $\boldsymbol{\mu}_L$ of the whole electronic shell:

$$\boldsymbol{\mu}_L = \boldsymbol{\mu}_{l1} + \boldsymbol{\mu}_{l2} + \ldots\ldots\ldots = \gamma_l \cdot \{\mathbf{P}_{l1} + \mathbf{P}_{l2} + \ldots\} = \gamma_l \cdot \mathbf{P}_L \qquad (3)$$

here $P_L = \mathrm{h}\sqrt{L(L+1)}$, where P_L – total orbital mechanical moment of atom, L – orbital quantum number of atom.

The spin magnetic moment $\boldsymbol{\mu}_s$ of electron is related with its mechanical moment by a relation:

$$\boldsymbol{\mu}_s = \gamma_s \cdot P_s, \qquad (4)$$

where $P_s = \mathrm{h}\sqrt{s(s+1)}$ – intrinsic mechanical moment of electron, s – spin quantum number, and $\gamma_s = e/m_0c$ – its spin gyromagnetic ratio. As one can see it twice the similar quantity for orbital motion: $\gamma_s = 2\gamma_l = 2e/2m_0c$. This fact was called the gyromagnetic anomaly and though there is no anything abnormal from the present point of view this term is used until now.

The sum of spin magnetic moments of all electron shells forms the total spin magnetic moment of atom $\boldsymbol{\mu}_S$:

$$\boldsymbol{\mu}_S = \boldsymbol{\mu}_{s1} + \boldsymbol{\mu}_{s2} + \ldots\ldots\ldots = 2\gamma_l \cdot \{\mathbf{P}_{s1} + \mathbf{P}_{s2} + \ldots\} = 2\gamma_l \cdot \mathbf{P}_S \qquad (5)$$

where $P_S = \hbar\sqrt{S(S+1)}$ – total spin mechanical moment of atom, S – spin quantum number of atom.

If we replace the quantities in equations (1) and (4) with the corresponding values then we will obtain the following relations for the orbital and spin magnetic moments of electron:

$$\mu_l = \frac{e}{2m_0c}\hbar\sqrt{l(l+1)} = \mu_0\sqrt{l(l+1)},$$

$$\mu_s = \frac{e}{m_0c}\hbar\sqrt{s(s+1)} = 2\mu_0\sqrt{s(s+1)}$$

The quantity $\mu_0 = \left|\frac{e\hbar}{2m_0c}\right| = 9.27\cdot10^{-21}\,\text{erg/oersted}$ is called the Bohr's magneton and serves as unit for measurements of the nuclear magnetic moment.

The quantum numbers l and s of an electron take the following values:

$$l = 0, 1, 2... (n-1); s=1/2,$$

where n – principal quantum number.

This means that the spin magnetic moment of electron is approximately equal to two Bohr magnetons:

$$\mu_s = 2\mu_0\sqrt{s(s+1)} = \mu_0\sqrt{3} \approx 2\mu_0,$$

while its orbital magnetic moment has the values, that are different for different states of electron in the atom, at that for $l = 0$

$$\mu_l = \mu_0\sqrt{l(l+1)} = 0.$$

The magnetic moments $\boldsymbol{\mu}_l$ and $\boldsymbol{\mu}_s$ are antiparallel oriented relative the corresponding mechanical moments $\boldsymbol{P}_l$ and $\boldsymbol{P}_s$, since the electron charge is negative (see Fig.1).

The directions $\boldsymbol{\mu}_l$ and $\boldsymbol{\mu}_s$ relative each other (the same as directions of quantum vectors in general relative the given axis in space) are determined by the space quantization rules: it is possible to specify precisely the projection value of quantum vector to the given axis, but it is impossible to determine simultaneously the other components of this vector. The projections of the orbital and spin magnetic moments

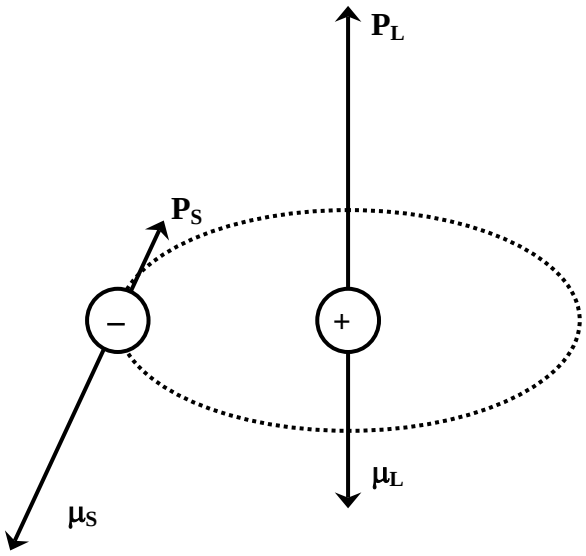

Fig. 1. Mechanical and magnetic orbital ($\mathbf{P_L}$, $\boldsymbol{\mu}_\mathbf{L}$) and intrinsic (spin, $\mathbf{P_S}$, $\boldsymbol{\mu}_\mathbf{S}$) moments of electron in the atom

of electron on the axis specified by direction of constant magnetic field **H**, are equal to:

$$\mu_{lH} = \mu_l \cdot cos\,(\boldsymbol{\mu}_l \boldsymbol{H}) = -\mu_0 m_l, \quad \mu_{sH} = \mu_s \cdot cos\,(\boldsymbol{\mu}_s \boldsymbol{H}) = -2\,\mu_0\, m_s,$$

respectively, where $m_l = -l; -(l-1,); \ldots + (l-1); +l$ – orbital magnetic quantum number of electron (quantum number of the orbital mechanical moment projection); $m_s = \pm 1/2$ – its spin magnetic quantum number (quantum number of the spin mechanical moment projection). The sign "minus" appears because the mechanical and magnetic moments of electron are opposite (the electron charge is negative).

Thus, the orbital magnetic moment $\boldsymbol{\mu}_l$ can have $2l+1$ different orientations relative the field **H**, and its projection μ_{lH} has $2l+1$ possible values.

The vector $\boldsymbol{\mu}_s$ is aligned either along **H** or reverse and its projection μ_{sH} toward the field is equal to μ_0 and $-\mu_0$, respectively.

The sum of the total orbital $\boldsymbol{\mu}_L$ and spin $\boldsymbol{\mu}_S$ magnetic moments of atom determines its total magnetic moment:

$$\boldsymbol{\mu}_J = \boldsymbol{\mu}_L + \boldsymbol{\mu}_S = \gamma_L \cdot \{\boldsymbol{P}_L + 2\boldsymbol{P}_S\}. \qquad (6)$$

Since the total mechanical moment of atom is equal to:

$$\boldsymbol{P}_J = \boldsymbol{P}_L + \boldsymbol{P}_S, \qquad (7)$$

where $P_J = \hbar\sqrt{J(J+1)}$ (J – quantum number of the total mechanical moment of atom) then it follows from (6) and (7) that the vector $\boldsymbol{\mu}$ makes an angle with vector $\boldsymbol{P}_J$ which differs from 180^o (as a result of the gyromagnetic anomaly).

A sketch of composition of moments $\boldsymbol{\mu}_L$ and $\boldsymbol{\mu}_S$ into the resulting magnetic moment $\boldsymbol{\mu}$ of all electronic shells is shown on Fig.2 (according to selected scale on Fig.2 the length of vector $\boldsymbol{\mu}_L$ is equal to length of vector $\boldsymbol{P}_L$: in this scale as a result of the gyromagnetic anomaly the length of vector $\boldsymbol{\mu}_S$ is twice the length of $\boldsymbol{P}_S$).

However, the physical meaning has only its component $\boldsymbol{\mu}_J$ along $\boldsymbol{P}_J$ but not the vector $\boldsymbol{\mu}$.

Thus, the effective magnetic moment of atom (or simply the magnetic moment

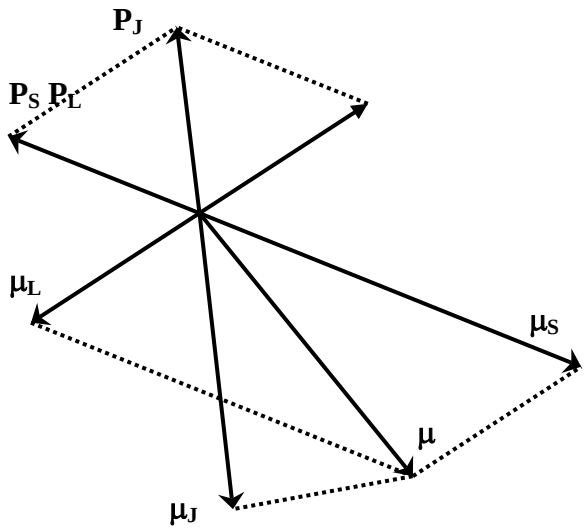

Fig. 2. Composition of the mechanical and magnetic moments of electronic shell of atom

of atom) $\boldsymbol{\mu}_J$ is antiparallel to $\boldsymbol{P}_J$ and numerically is equal to:

$$\mu_J = \mu_L \cdot \cos(\boldsymbol{\mu}_l \boldsymbol{P}_J) + \mu_S \cdot \cos(\boldsymbol{\mu}_S \boldsymbol{P}_J).$$

Simple algebra (see Fig.2) gives:

$$\mu_J = \mu_0 g_J \sqrt{J(J+1)}, \qquad (8)$$

where

$$g_J = 1 + \frac{J(J+1) + S(S+1) - L(L+1)}{2J(J+1)} \qquad (9)$$

– is the so-called Landé splitting factor, g-factor, or factor of spectroscopic splitting of the electronic shell of atom. From (9) it follows that the value of Landé splitting factor depends on state of atom. It is possible to make the qualitative conclusion about the origin of magnetism of the given atom from the values of this factor: if $g_J = g_L = 1$, it is possible only at $S=0$, in this case $\mu_S = 0$, and magnetism is created only due to the orbital motion of electrons: if $g_J = g_S = 2$ (to be more precise 2.00238) then it is possible for $L=0$ ($\mu_L = 0$), and magnetism has pure the spin origin. Certainly the intermediate cases are possible.

In case of condensed matter when the interaction of the given atom with atoms of substance can be considerable, the g-factor can differ from that given by equation (9). These differences give the possibility to evaluate both the character of the interactions of atoms, and the origin of magnetism of the given substance.

If we deal with atom or ion with partially filled shell that is characterized by the principal and orbital quantum numbers n and l, then, since the orbital moments and spins of electrons can be differently oriented, it is possible to obtain a set of various states (terms) of atom or ion, each of which would have its own value of quantum numbers L, S and J of the total moments. Each of terms will have its own energy. Since any system in the absence of external actions tends to occupy a state with the lowest energy, only a term with the lowest energy is populated (the energy gap between the lowest and the first excited term, as a rule, considerably exceeds the energy of thermal motion at temperatures of the order of hundreds Kelvin).

It is possible to choose a term from all possible terms of atom or ion with the lowest energy using the well-known empirical rules established by Hund in 1927. According to these rules, the lowest energy has the term with the largest (with the given electronic configuration of atom or ion) value of the total spin S and the largest (at this S value) total orbital moment L. If L and S are not equal to zero and if in a layer n of shell l there are less than half of the maximum possible number of electrons ($<2l+1$), then the level of a multiplet with $J = |L-S|$ has the lowest energy, and at the number of electrons larger than $2l+1$ – level with $J = L+S$.

The Hund's rule can be formulated also as follows:

1) The total spin quantum number $M_S = \Sigma(m_s)_k$ in the ground state has a maximum within the limits allowed by the Pauli's exclusion principle.

2). The total orbital quantum number $M_L = \Sigma(m_l)_k$ in the ground state has a maximum within the limits allowed by rule 1.

3). The total value of quantum number of the total moment J for partially filled shell is given by expressions:

$J = |L-S|$ if the shell is less than half filled,

$J = L+S$ if the shell is more than half filled.

Let's consider the application of Hund's rules with the Mn^{2+} ion as an example, having the electronic configuration of the open shell $3d^5$ (in the layer n=3 there are 5 electrons with the orbital quantum number l = 2; we remind that the value of number l is designated by letter d). According to the Pauli's exclusion principle there shall be no two electrons with identical quantum numbers n, l, m_s and m_l in the atom. Since n and l for all five electrons are identical, there shall be no two electrons with identical pairs of numbers m_s and m_l in a shell. The total spin of the ion will be maximal, if the spins of separate electrons are oriented equally, i.e. if m_s=1/2 for all electrons; then M_S = 5/2 and S = 5/2. But in that case the numbers m_l of all five electrons shall be different. Since m_l can have $2l$+1 values and l = 2, then m_l=2, 1, 0,-1,-2 for five electrons, and the total quantum number M_L=0, i.e. L=0. Finally, the total quantum number of the total moment $J = L+S$ = 5/2. So, the ground state of the Mn^{2+} ion is characterized by quantum numbers S = 5/2, L = 0, J = 5/2. The spectroscopic symbol of this term – $^6S_{5/2}$. Since L=0 in this state, the g-factor has, according to relation (9), the value g=2. Since L=0 and $J = S$ for the Mn^{2+} ion, the ion is frequently characterized by the number S instead of the number J.

To obtain the total and, consequently, exact value of the magnetic moment of atom in whole, μ_F, the quantity μ_J (6) shall be added to the vector value of the magnetic moment $\mu_{of\,I}$ of atomic nucleus:

$$\boldsymbol{\mu}_F = \boldsymbol{\mu}_L + \boldsymbol{\mu}_S + \boldsymbol{\mu}_I = \gamma_L \cdot\{\boldsymbol{P}_L + 2\boldsymbol{P}_S\} + \boldsymbol{\mu}_I.$$

The intrinsic magnetic moment of nucleus is equal to $\boldsymbol{\mu}_I = \gamma_I \cdot \boldsymbol{P}_I$, where γ_I - gyromagnetic ratio for nucleus equal to $\gamma_I \cdot = g_I\, e\, /\, (2m_p c)$; g_I - its spectroscopic splitting factor, m_p - mass of proton, $\boldsymbol{P}_I$ - intrinsic angular momentum of nucleus, numerically equal to $P_I = \mathrm{h}\sqrt{I(I+1)}$, where I - spin quantum number of the nucleus.

Using definitions of γ_I and $\boldsymbol{P}_I$ let's determine the value of the intrinsic magnetic moment of nucleus: $\mu_I = \mu_{0I}\, g_I \sqrt{I(I+1)}$.

The quantity $\mu_{0I} = \left|\frac{e\mathrm{h}}{2m_p c}\right| = 5.05 \cdot 10^{-24}$ erg/oersted is called the nuclear magneton and serves as unit for measurement of the magnetic moments of nuclei.

Since μ_{0I} is approximately 2000 times smaller than μ_0 (Bohr magneton) the nuclear magnetic moments are approximately 2000 times smaller than the electronic magnetic moments (g_I and I^* are of the order of unity). Therefore the nuclear magnetism can be often omitted. However "often" does not mean "always": in some cases it is impossible to neglect the nuclear magnetism. For example, in EPR it causes occurrence of the hyperfine structure of the absorption resonance lines. Moreover, the existence of nuclear magnetic moments provides possibility for very important version of magnetic resonance – a nuclear magnetic resonance.

2. Behavior of the magnetic moments in the magnetic fields and the nature of paramagnetic resonance

To understand the physics of electron paramagnetic resonance the two approaches are possible:

a) classical, on the basis of consideration of a nuclear magnetic moment motion in the external field as the classical mechanical system with properties of a top and capable to change its energy under the action of variable part of field;

b) quantum mechanical, on the basis of representation with the energy level splitting of the atom having a magnetic moment, in a static magnetic field with a set of the Zeeman sublevels, between which the transitions are possible under the influence of a high-frequency magnetic field.

Both approaches give the same results in the sense that they allow to formulate the same basic laws of the phenomena.

A. Magnetic field **H** acts on atom as on a regular magnet, orienting its magnetic moment so that the energy of their interactions:

$$\Delta E_H = -\boldsymbol{\mu}_J \boldsymbol{H} = -\mu_J H \cos(\boldsymbol{\mu}_J \boldsymbol{H}) \qquad (10)$$

would be the lowest. This requirement will be satisfied if $\boldsymbol{\mu}_J$ orients along **H**. However the achievement of this is prevented by the gyroscopic properties of atom: the field **H** is unable to orient $\boldsymbol{\mu}_J$ parallel to it, and it will cause precession of the magnetic moment of atom with the Larmor frequency. It is necessary, however, to take into account that not only the atom as a whole has the gyroscopic properties, but also any electron separately since it has the mechanical moment $\boldsymbol{P}_s$. In the magnetic field **H** the magnetic moment of every electron of atom shall precess with the Larmor frequency, but different from the precession frequency of the magnetic orbital moments, since the gyromagnetic ratio for the spin of electron is twice for orbital motion. As a result the atomic magnetic moment $\boldsymbol{\mu}_J$ will precess in the magnetic field H with the frequency:

$$\omega_0 = \gamma H = g_J \frac{eH}{2m_0 c}, \qquad (11)$$

where g_J – Landé splitting factor, which value is given by equation (9), also depends on the contribution of the orbital and spin moments to the total magnetic moment of atom.

Proceeding from the circular frequency to the linear one, equation (11) may be written as follows:

$$\nu_0 = g_J \frac{eH}{4\pi m_0 c}, \tag{12}$$

and if we substitute here the values of constants then we will find:

$$\nu_0 = 1.3995 \cdot 10^6 g_J H \text{ [Hz]}, \tag{12a}$$

that for $H = 10^3$-10^4 Oersted corresponds the centimeter band of radio waves.

Now suppose that the atom is affected not only by the static magnetic field **H**, but also by weak field $\mathbf{H}_\nu$ rotating with frequency ν in a plane, perpendicular to **H** (see Fig.3).

If frequency $\boldsymbol{\nu}$ coincides with frequency $\boldsymbol{\nu_0}$ (equations (12) and (12a)) then the vectors μ_J and $\mathbf{H}_\nu$ rotate synchronously and stationary relative each other. But in this case the field $\mathbf{H}_\nu$ will act on μ_J as any magnetic field acts on a magnetic moment: it will tend to orient the vector μ_J parallel to it. This means that the mechanical moment **N** affects the atom, deviating the magnetic moment μ_J from its initial direction and increasing the energy of its interaction with the field **H** at the expense of energy of the variable field $\mathbf{H}_\nu$.

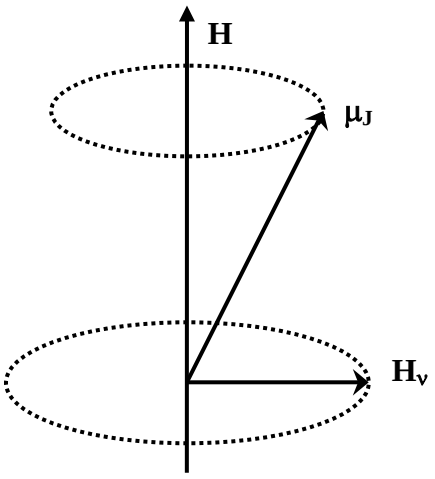

Fig. 3. Behavior of the atomic magnetic moment $\boldsymbol{\mu_J}$ in the static **H** and the high-frequency magnetic fields $\mathbf{H}_\nu$

The described interaction of the atomic magnetic moment with the high-frequency (rotating) magnetic field is realized only at the coincidence of rotation of vector $\mathbf{H}_\nu$

with the Larmor precession of the moment μ_J in the field **H** both on frequency and on direction; thus, this interaction has a resonant character. Really, imagine that the frequencies ν and ν_0 are different or their rotation directions are opposite. Then the relative position of μ_J and $\mathbf{H}_\nu$ will change continuously, consequently the direction of the moment **N** will change: it will periodically increase or reduce the angle between μ_J and the field **H**. In average the effect of field $\mathbf{H}_\nu$ on the magnetic moment μ_J will be equal to zero. This, by the way, gives the possibility to use in the real experiment the sinusoidal linearly polarized field with the same frequency instead of the rotating magnetic field $\mathbf{H}_\nu$. The enquiry is that this linearly polarized field is the sum of two oppositely rotating fields with half amplitude compared with a sinusoidal field. The corresponding resonance interaction of $\mathbf{H}_\nu$ with μ_J will be realized by the one of two specified components that rotates in precession direction of moment μ_J.

The stated mechanism of the magnetic moment μ_J deviation by the high-frequency field $\mathbf{H}_\nu$ from the equilibrium position and the energy of moment μ_J related to it in the field **H** does not explain completely the reason of energy absorption of the field $\mathbf{H}_\nu$ by the magnetized paramagnetic substance. Really, in the field **H** the moment μ_J has the lowest energy if it is parallel to a field; deviating from this orientation at the effect of field $\mathbf{H}_\nu$ this moment gains the energy. This is accompanied by energy absorption of the high-frequency field. As experiment shows, the high-frequency field energy is absorbed at EPR phenomenon continuously and arbitrarily long - while the substance is affected by the fields **H** and $\mathbf{H}_\nu$. Intuitively it is clear that the spin system is not capable to absorb energy interminably. So, to where this energy leaves?

The atoms of any substance are not isolated and are bound by interactions with each other. In paramagnetic crystals two of these interactions play the greatest role: the spin-spin and the spin-lattice interactions. The first one is interaction between the magnetic moments of atoms and by nature is quite similar to interaction of microscopic magnetic needles: it determines the processes of energy redistribution

inside the “spin system”, i.e. in all set of magnetic atoms of the given solids. This process equalizes the energy of the given atoms, it is called a spin relaxation, and the time necessary for its realization – the spin-spin relaxation time. This interaction not very strong, but plays the essential role in electron paramagnetic resonance: in case when it is realized between the electronic moments – it causes, considerably, the line width of the resonance absorption.

The second type of interaction is even more essential for all magnetic resonant phenomena as it causes the possibility of their existence. The spin-lattice interaction for a variety of paramagnets is very different by the physical mechanisms, but has the common features. It represents the process (better to say – processes) of energy exchange of the spin system with a crystal lattice as a whole and is reduced, ultimately, to transition of energy of a precessional motion of the magnetic moments into heat, in other words – into energy of oscillations of the atoms forming a lattice. This energy transmission of the spin system to a lattice requires a certain time; it is called a time of spin-lattice relaxation and strongly depends on temperature - increases with lowering of a temperature.

Now it is easy to understand, to where the energy of a variable magnetic field absorbed at electron paramagnetic resonance leaves. If we consider the behavior in the magnetic fields $\mathbf{H}$ and $\mathbf{H}_v$ of not a particular atom but the ensemble of atoms in a paramagnetic crystal it is necessary to take into account a spin-lattice interaction. The alternating field that deviate the magnetic moments of all atoms from the position of stable equilibrium increases the energy of the total spin system. The spin-lattice interaction transfers this energy to a lattice, increasing intensity of thermal vibrations of all its atoms (there can also be a nonmagnetic atoms among them), as a result of which the magnetic atoms return into their initial state and are ready to repeat again the process of transformation of an electromagnetic energy into heat. Certainly, it is not necessary to think that all magnetic atoms of a crystal do it synchronously. Actually such process has a statistical character: part of atoms deviated by a high-frequency field from the equilibrium accumulate the energy while the other transfers

the excess of energy to a lattice, and the third ones return to an equilibrium state. Thus, at each given moment of time there are the atoms in a crystal which are in any of possible stages of the described processes. As a result the paramagnetic crystal (and also any other paramagnet including the fluid) will continuously absorb energy of a variable magnetic field while the resonance requirements are met.

This is the phenomenon of electron paramagnetic resonance (EPR).

B. Quantum – mechanical description allows understanding of this phenomenon more precisely and in full and it is based on the following basic representations.

The energy, mechanical and magnetic moments of atom are quantized by value, i.e. can possess only certain values forming discrete sets, and the mentioned moments are quantized also spatially: they can be oriented relative, e.g., the external field **H** only with some well defined angles. Hence the natural conclusion follows: in the external magnetic field **H** each energy level of the paramagnetic atom will split on a series of sublevels. Really, the energy of interaction (10) of μ_J with **H** is equal to:

$$\Delta E_H = -\vec{\mu}_J \vec{H} = -\mu_0 g_J \sqrt{J(J+1)} H \cos(\vec{\mu}_J \vec{H}).$$

Due to space quantization the quantity

$$\sqrt{J(J+1)} \cos(\vec{\mu}_J \vec{H}) = M_J,$$

called the magnetic quantum number of atom can have only some values that form the following set:

$$M_J = -J; -(J-1); \ldots +(J-1); +J,$$

i.e. with the given J that determines the total mechanical moment of the electron shell of atom (see (7)) the magnetic quantum number can have any of $2J+1$ allowed values for it. Then

$$\Delta E_H = \mu_0 g_J H M_J, \qquad (13)$$

and this means also that the energy level of atom would split on $2J+1$ sublevels, the number of which is equal to the number of possible orientations of the moment of atom (see Fig.4).

From Fig.4 and (13) one can see that any neighboring two sublevels are separated by the equal energy intervals $\mu_0 g_J H$. The numbers N_1 and N_2 of the atoms that are on two any sublevels, separated by energy interval ΔE, in case of thermodynamic equilibrium are related through the well-known Boltzmann equation:

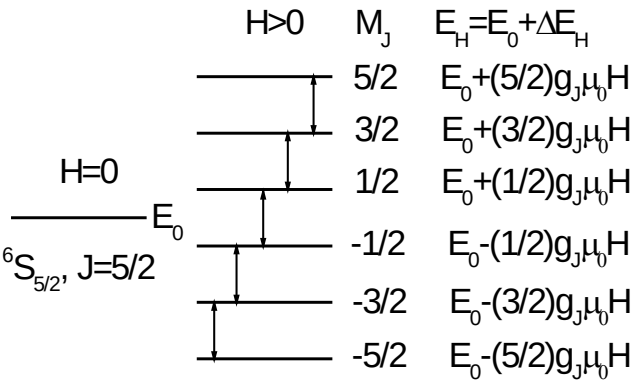

Fig. 4. Splitting of the basic term of the Mn^{2+} ion by the magnetic field **H**. The arrows indicate the allowed transitions between the levels.

$$N_2/N_1 = \exp(-\Delta E/kT).$$

It means that atoms of the paramagnetic crystal in the magnetic field **H** occupy the magnetic sublevels with different density: the less is the energy of the given sublevel the larger is the density on it.

If the paramagnet is affected by not only the field **H** but also by the high-frequency field $\mathbf{H}_\nu$ then the latter will flip the atoms from the lower levels on overlying ones and back if only the field frequency corresponds to the energy difference between the given sublevels:

$$h\nu = \Delta E. \qquad (14)$$

These types of transitions are governed by a simple selection rule: realizable only those transitions for which the magnetic quantum number changes on unity, i.e. $\Delta M_J = \pm 1$. Then the requirement (14) can be written as follows:

$$h\nu_0 = \Delta E = \Delta E' - \Delta E'' = \mu_0 g_J H (M_J'' - M_J') = \mu_0 g_J H \Delta M_J$$

or taking into account the selection rules:

$$h\nu_0 = \mu_0 g_J H, \quad \nu_0 = g_J \frac{\mu_0 H}{h} = g_J \frac{eH}{4\pi m_0 c}.$$

Thus the quantum – mechanical description leads to the same frequency of the resonance transition as that given by the classical description.

The high-frequency magnetic field $\mathbf{H}_\nu$ transfers the atoms predominately from the lower levels to the upper ones at the expense of some part of its energy when the resonance conditions are met. As a result of spin-lattice interaction the particles of top levels transfer the excess energy to a lattice and jump without energy radiation again to the lower levels. At the continuous effect of the magnetic fields there is a dynamic balance between the atoms that elevate on top levels and leaving down to the lower levels. The energy of the high-frequency magnetic field will be continuously absorbed by the substance, thus heating it up.

From the aforementioned it is clear that the electron paramagnetic resonance is related to the Zeeman effect in optics. The difference is that at Zeeman effect the transitions are top-down between the magnetic sublevels of various atomic levels, i.e. with emission of electromagnetic energy in the range of high (optical) frequencies. In case of electron paramagnetic resonance such transitions are realized top-down between the sublevels of the same atomic level and are accompanied by electromagnetic energy absorption in the range of the lower frequencies.

3. Basic characteristics of the electron paramagnetic resonance spectrum

Complex and diverse interactions in the paramagnetic substance determine the essential features of behavior of the atomic magnetic moments in the fields **H** and $\mathbf{H}_\nu$ and thus determine the character of the resonant magnetic absorption spectrum. The spectra for the various magnetic atoms in different substances appear rather various

and sometimes rather difficult and containing a lot of lines with different intensities and line shapes.

3a). Width and intensity of the resonance lines

It is known that the spectroscopic lines are never infinitely narrow. The finite width of a line and the shape of its contour are caused by tailing of the atomic energy levels between which the given transition occurs by effect of the various physical factors among which the interactions between the radiating atoms have the greatest importance.

When discussing a problem of emission or absorption line width it is necessary to take into account first of all the following factor for the problem - broadening of energy levels due to the uncertainty principle: if the atom is on the given energy level for the time period Δt then the value of energy of this state will be within the limits of the band ΔE_r determined by a relation:

$$\Delta E_r \Delta t \approx \hbar.$$

Therefore, even in the conditions of total absence of the interatomic interaction the spectroscopic line has the finite, the so-called natural width:

$$\Delta \nu_{Nat} = 1 / (2\pi\Delta t), \qquad (15)$$

determined by a lifetime of spontaneously emitting atom in the excited state (i.e. on the upper energy level). This remains valid in the presence of interactions between emitting (absorbing) atoms or their environment when the lifetime of atom Δt on the initial level is determined by these interactions. It is easy to show that in these cases the atom lifetime is shortened, broadening of the energy levels increases and the spectrum line width considerably exceeds the "natural" one, and, as well as for this latter it is given by equation (15).

As it was already mentioned above, the basic types of interactions in the case of magnetic resonance are the spin-spin and spin-lattice interactions. Having designated

the corresponding relaxation times T_1 and T_2, respectively, for the EPR absorption line widths on the basis of the equation (15) it is possible to write:

$$\Delta\nu = 1 / (2\pi T_1) + 1 / (2\pi T_2). \qquad (16)$$

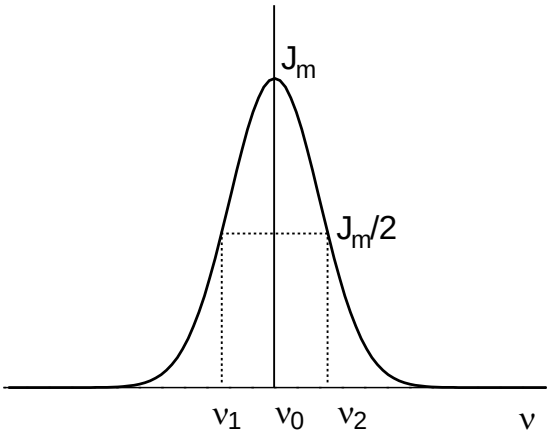

Fig. 5. The width and intensity of the absorption line.

This relation qualitatively and correctly describes the line widths and a very important conclusion about possibility of EPR observation in pure condensed paramagnets follows from it. In these substances all atoms have the magnetic moments and they are located very closely - at the distances determined by a lattice period. The spin-spin interactions are very strong, the energy exchange between atoms is very fast, the relaxation time T_2 is very small, and the resonance line width is determined, mainly, by the second term in (16) and is very large. Thereby, the weaker interactions - spin-lattice interactions and interactions of atomic electrons with a nucleus - actually will not affect the shape of the resonance spectrum. Therefore EPR study on pure paramagnets is less informative and is not interesting. The real value and development was obtained by EPR starting from research of magneto-diluted substances, especially the crystals which paramagnetic properties are created by small impurity of paramagnetic atoms (ions) in a diamagnetic lattice. There is a large number of these crystals of a natural origin, for example, a ruby (Al_2O_3), containing the paramagnetic triple-charged ions of chrome in small concentrations and replacing the aluminium ions in a diamagnetic lattice of corundum; calcite ($CaCO_3$), containing

usually the doubly charged ion of manganese as a paramagnetic impurity; diamond that contains many of paramagnetic impurities: nitrogen, aluminium, iron ions, etc. A particular role was played among these crystals by ruby: an important area of the up-to-date technical physics, quantum radio electronics has begun with research of its radiospectroscopic properties. The requirements arisen in this connection had led to development of the industry of the artificial paramagnetic impurity crystals, including a ruby, superior compared with natural crystals.

Quantitatively the width of the absorption resonance line is measured by difference of the frequencies $\Delta\nu = \nu_2 - \nu_1$ between points of a line contour, taken at half of its height (Fig. 5).

The integrated intensity of a line is measured by the area limited by its contour and the frequency axis. The amount of the absorbed energy is proportional to the difference of level populations between which the given transition occurs. At the given frequency and temperature this difference is proportional to the total number of magnetic atoms in the test sample that allows to measure the concentration of magnetic ions in the given substance from the integrated intensity of the absorption line.

3b). EPR line shapes

The EPR line shapes can be rather various at their identical integrated intensity. Various types of interactions cause not only a different line broadening, but also cause difference of their shapes. For EPR spectra the most typical are the Gaussian and Lorentz line shapes. From Fig. 6, where these lines and their derivatives are presented, it is clear that the Lorentz line is narrower at the center, but is wider on the "wings", compared with the Gaussian line, and their width at the half height is different. We omit here the equations describing the mentioned types of lines and mention only that the Gaussian shape line is observed in cases of strong domination

of the spin-spin interaction in a paramagnet over the spin-lattice interaction, and the Lorentz line - at inverse relation of these interactions.

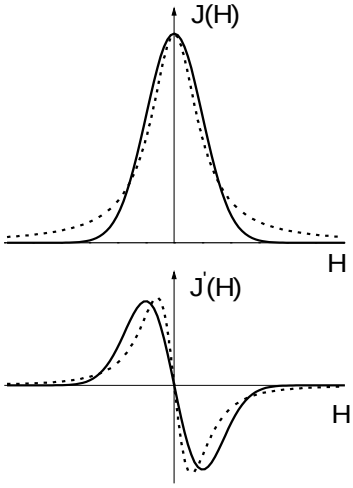

Fig. 6. The absorption line shape and its derivative:
solid line – Gaussian shape line;
dotted line – Lorentz shape line.

3c). Fine structure of the EPR spectrum

As it is evident from equations (13), (14) and Fig. 4, the intervals between the neighboring Zeeman sublevels of system of noninteracting atoms are identical and the allowed transitions between them in the given field **H** occur at the same frequency, i.e. give the same absorption line. The pattern will be essentially different when the magnetic atom (ion) with the magnetic quantum number $J>1/2$ is a part of solid substance and is strongly affected by the environment. Both in a crystal and in amorphous substance there exist a strong internal electric fields created by the neighboring ions and affecting the magnetic ion so that its energy levels are split (this is the Stark effect known from optics).

Let's consider the influence of a crystal field with the manganese ion in a calcite ($CaCO_3$) as an example. The Mn^{2+} ion has five unpaired electrons giving the total spin magnetic moment $\mu_S = (35)^{1/2}\mu_0$. The magnetic spin number M_J (or M_S, as it was

already mentioned, it is the same for Mn^{2+} ion) has six different values: ±5/2; ±3/2; ±1/2. (The divalent manganese ion has zero orbital moment and, hence, does not make the contribution to EPR. For the other ions of the transitional elements as it will be established below, the orbital magnetic moment will also do not make any contribution to EPR because of "freezing of orbits" effect). The effect of crystal field leads to splitting of the energy levels of the ion already at H=0 on three Stark sublevels. At superposition of the external magnetic field H each of these sublevels split on two Zeeman sublevels. At that the effect of the crystal field leads to various shifts of Zeeman sublevels (owing to Stark effect), to violation of equality of the energy intervals between them. Therefore the transitions between the sublevels in the same field H will occur at various frequencies, the absorption line splits into group of lines (according to the selection rules $\Delta M_S = \pm 1$ - on five lines; see Fig. 7(a))

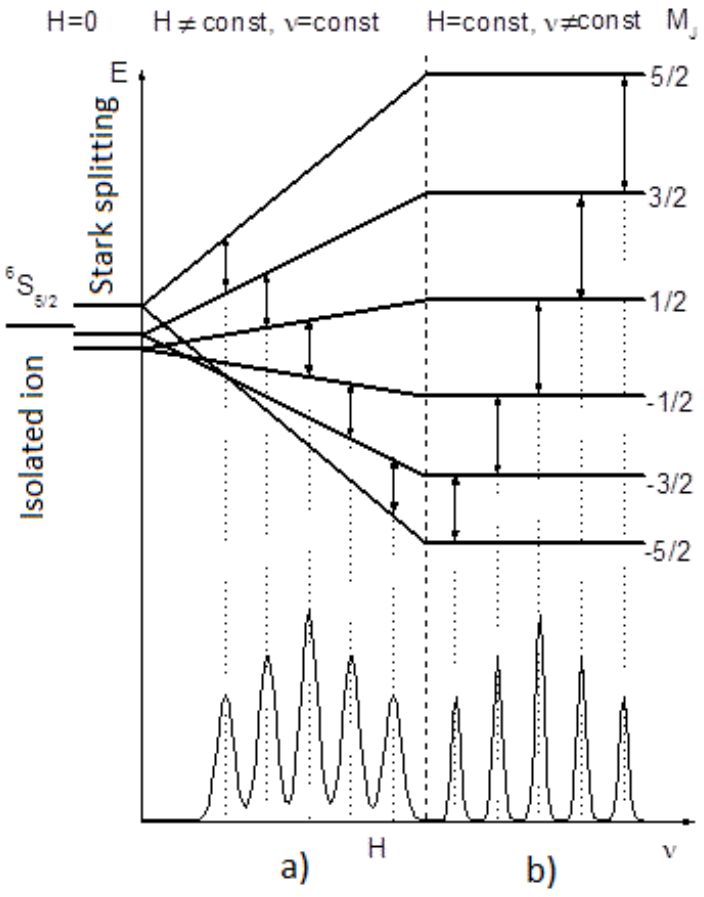

Fig. 7. Fine structure of EPR line of Mn^{2+} ion in $CaCO_3$

This splitting of EPR line by the crystal field is called the fine structure of the EPR-spectrum. It is more convenient to explore the EPR- spectrum experimentally at constant frequency ν of a high-frequency electromagnetic field and slow varying with time the magnetizing field *H*. The transitions between the Zeeman sublevels of an ion in this case occur also only at a resonance, i.e. at coincidence of frequency ν of the high-frequency field $\mathbf{H}_\nu$ with ν_0 - frequency of the quantum, absorbed at transition between the neighboring sublevels ($\Delta M_S = \pm 1$). But because of effect of the crystal field the equality of the energy intervals between the sublevels of the Mn^{2+} ion is broken, the transitions between the neighboring sublevels will occur only at the moments of time when the field *H* will have the intensity, at which

$$\nu_0 = g_{кр}^{\,i}\, eH / (4\pi mc) = \nu$$

($g_{кр}^{\,i}$ - spectroscopic splitting factor of the neighboring sublevels of ion in the field of a lattice), i.e. at five various values of the field *H* (see Fig. 7 (b). Thus, as a result we will observe the fine structure of the EPR line - the absorption line will consist of group of lines (five lines).

The crystal field causes also two rather important effects: the so-called "freezing" of the orbital moments and angular dependence of a resonant spectrum. The first effect is that the strong crystalline field, affecting a moving electron in an atom, spatially fixes its orbit and therefore the orbital magnetic moment cannot react at the external magnetic field and ceases to take part in the process of electron paramagnetic resonance. Meanwhile, the spin magnetic moment of electrons is not affected by electric field of a crystal and as in case of the free atom it is freely oriented in the field H according to the rules of spatial quantization. It causes all features of electronic paramagnetic resonance.

The second effect is related to symmetry of the internal electric field of the crystal that depends on lattice symmetry of the latter. The magnetic field H, acting on an ion with different angles relative a crystal field, splits differently its energy levels owing to what the position and the number of the resonance lines will depend on the

angle θ between **H** and crystal axes. In the first approximation the dependence of distances (along the field **H** at fixed frequency ν_0) versus the specified angle is described by the function $(3\cos^2\theta - 1)$.

Examination of the fine structure of the EPR-spectrum gives a lot both for understanding the properties of a paramagnetic ion and for opinion about features of the crystal field and its symmetry.

The character of interactions of the paramagnetic ion with its diamagnetic environment can be such that observation either of a single line or a fine structure can be impossible in usual conditions: thermal oscillations of the crystal lattice widen the line so that it is necessary to cool down the crystal to the possible lowest (liquid helium or nitrogen) temperatures for their observation.

The fine structure of EPR spectrum is observed only when there is the electric anisotropy of the crystal lattice, i.e. the symmetry of charges surrounding a paramagnetic ion is low enough. If the surrounding ions are located with high symmetry it may happen that the fine structure of the EPR spectrum will be absent. This appears, for example, for the case of the Mn^{2+} ion, replacing the Ca^{2+} ions in a fluorite crystal (CaF_2). The Mn^{2+} ion is located at cube center in which corners the F^- ions are located. The crystal electric field in the location of the manganese ion has high, cubic symmetry, and the fine structure of manganese spectrum is absent. Thus, the EPR Mn^{2+} spectrum in crystal CaF_2 should consist of one line, as for the free ion (Fig. 4).

3c). Hyperfine structure of EPR spectrum

The very essential feature of EPR spectra in many cases is the hyperfine structure appearing, as in the case of optical spectra, as a result of interaction of the magnetic moments of unpaired electrons with the magnetic moment of nucleus. We will examine this using the manganese ion in fluorite as an example.

The spin of manganese nucleus is equal to $I = 5/2$. This means that in the

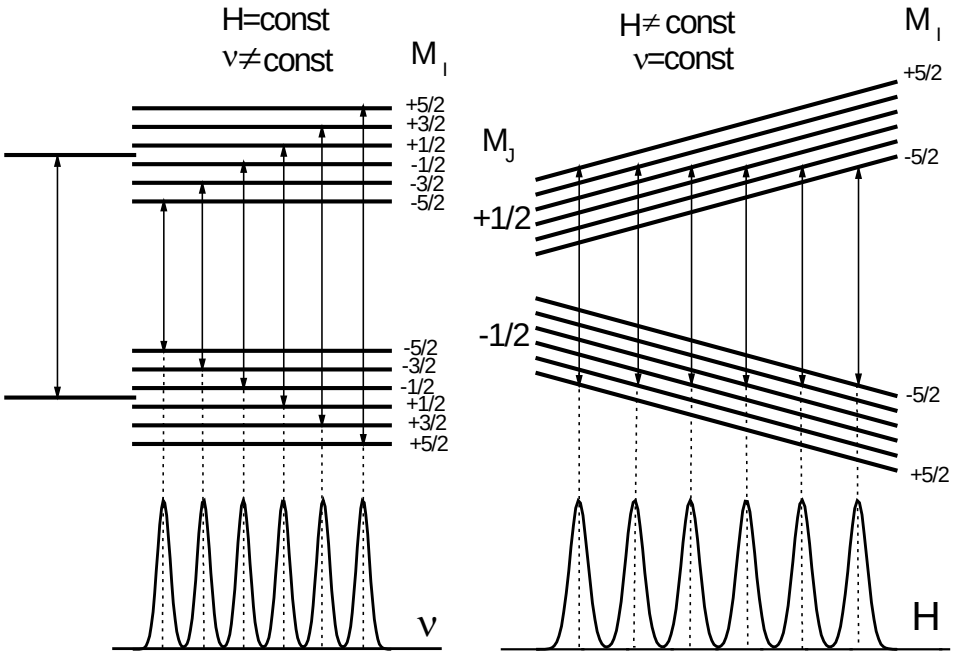

Hyperfine splitting of levels M_J=1/2 and M_J =-1/2 of the ion Mn^{2+} and transitions between them.

external field H the magnetic moment of nucleus can take $2I+1 = 6$ various directions. And this, in turn, means that the electronic magnetic moment will be affected by the total magnetic field $\mathbf{H}+\mathbf{H}_I$, able to take six various values. In this field the magnetic moment μ_S (or μ_J) will have six possible values of energy and as a result each of the electronic Zeeman sublevels will split on six sublevels of a hyperfine structure. As affected by the high-frequency field H_ν the transitions will appear

governed by the following selection rules: $\Delta M_S = \pm 1$: $\Delta M_I = 0$ (the nuclear moment at the time of electronic transition does not change its orientation). As a result the given EPR line of the fine structure will split on six components (see Fig. 8).

A manganese ion in a calcite, as we saw, has five lines of the fine structure; each of them will split on six lines of the hyperfine structure. Hence, the EPR spectrum of the Mn^{2+} ion in a calcite will consist of thirty lines of absorption. Unlike for a calcite, the EPR spectrum of the Mn^{2+} ion in fluorite will have no fine structure, i.e. will consist only of six lines of a hyperfine structure.

Research of hyperfine structure of EPR line gives the possibility to determine the spin of a nucleus of a paramagnetic ion, allows to evaluate the state of its unpaired electrons.

PROCEDURE AND TECHNICS OF EXPERIMENT

1. EPR radio spectrometers

Radio spectrometers of various types are used for recording the EPR spectra.

EPR spectrometers can be subdivided by methods of signal amplification into the following types:

1) video spectrometer with low-frequency signal amplification;

2) radio spectrometer with double modulation of the magnetic field, resonant amplification and synchronous detection at the second modulation frequency;

3) superheterodyne spectrometer with intermediate frequency amplification.

Sensitivity is the prime parameter of radio spectrometers.

The minimal number of the paramagnetic centers detected by a spectrometer in the absence of the saturation effect without account of intrinsic noises of the measuring circuit is equal to: $N_{\min} = \frac{\alpha}{Q_0 V}\sqrt{\frac{kT\Delta f}{P_0}}$,

where α - constant depending on type of the device; Q_0 - resonator quality factor (Q-factor); V - effective volume of the test sample; Δf - pass band of a measuring track; P_0 - microwave power.

At the same conditions: identical power of the radio-frequency field (of the order of units of the milliwatt), Q-factor of the resonator, effective volume of the test sample, etc., a superheterodyne radio spectrometer shows the greatest sensitivity, the least - video spectrometer.

The problem of the sensitivity determination of any installation is rather difficult, since not only the test sample parameters (EPR line width, configuration of the sample, etc.) are of importance. Therefore the majority of experimentalists determine the sensitivity of the installations on the substance called $\alpha\alpha$'-diphenyl-β-picrylhydrazyl (2,2-diphenyl-1-picrylhydrazyl) (DPPH). Take the known batch of this radical and by measuring a signal-to-noise ratio determine the sensitivity of the installation. The spectrometer sensitivity enhances with frequency step-up of a spectrometer. In average the sensitivity of various types of the spectrometers of a three-centimeter band (X-band, frequency 10 GHz) is as follows: superheterodyne spectrometer – 10^{11}-10^{12}, spectrometer with double modulation – 10^{10}-10^{11}, video spectrometer – 10^{14}-10^{16} magnetic centers per volume unit.

2. Description of Varian E-12 EPR-spectrometer

Radio spectrometer EPR E-12 of a three-centimeter band (X-band with frequency around 9.5 GHz) is intended for observation and recording on a plotter the EPR spectra of the free radicals, paramagnetic ions, radiation damage centers and other paramagnetic particles.

The frequency of a microwave field at which there is an energy resonance absorption by the paramagnetic sample (EPR frequency), as it is known, is related to

the value of static magnetic field into which the sample is placed by the following relation:

$$h\nu = \mu H_0 \qquad (17)$$

Thus, it is evident that the resonance absorption line can be observed at change of the microwave field frequency and constant value of the magnetic field or at change of the magnetic field value and constant frequency of the microwave field. In radio spectrometer E-12, as well as in general in EPR spectrometers, the second variant of observation of resonance absorption of the microwave field energy by substance is used.

The graphic lines of the absorbed microwave energy by the sample registered by a radio spectrometer *versus* intensity of the static magnetic field affecting the sample is the EPR spectroscopic lines of substance.

Spectrometer E-12 is the EPR-spectrometer of reflective type. The block diagram of EPR-spectrometer E-12 is shown on Fig. 9.

Klystron generator (1) is used as the source of the energy in the microwave range which frequency can change within a small band 8.8 – 9.6 GHz. The microwave energy of the klystron generator enter into a spectrometer waveguide transmission line through a gate (2) that prevents hit back of microwave energy into a klystron, reflected from a loading that can lead to malfunctions in generator operation. The microwave energy, entering into the transmission line, if necessary, can be attenuated on 30 dB (1000 times) by means of the step attenuator (3). The smooth change of power is carried out by the adjustable attenuator (4). Hitting on the circulator (5), the microwave energy is directed to the rectangular resonator (6) in which it excites the oscillations H_{102} through a coupling aperture. Changing the dimensions of a coupling aperture, it is possible to match the resonator with a waveguide that brings microwave energy to it, i.e. to achieve, that energy hitting on the resonator would completely, without reflection, be absorbed by the resonator and dissipated in it. Usually it is not necessary to achieve full matching of the resonator with a waveguide: part of the power should reflect from the resonator and, having

transited through the circulator (6), hit on the microwave detector (7), creating a current of 200-250 μA in it. In this case the detector will work in the linear mode and have the maximum sensitivity.

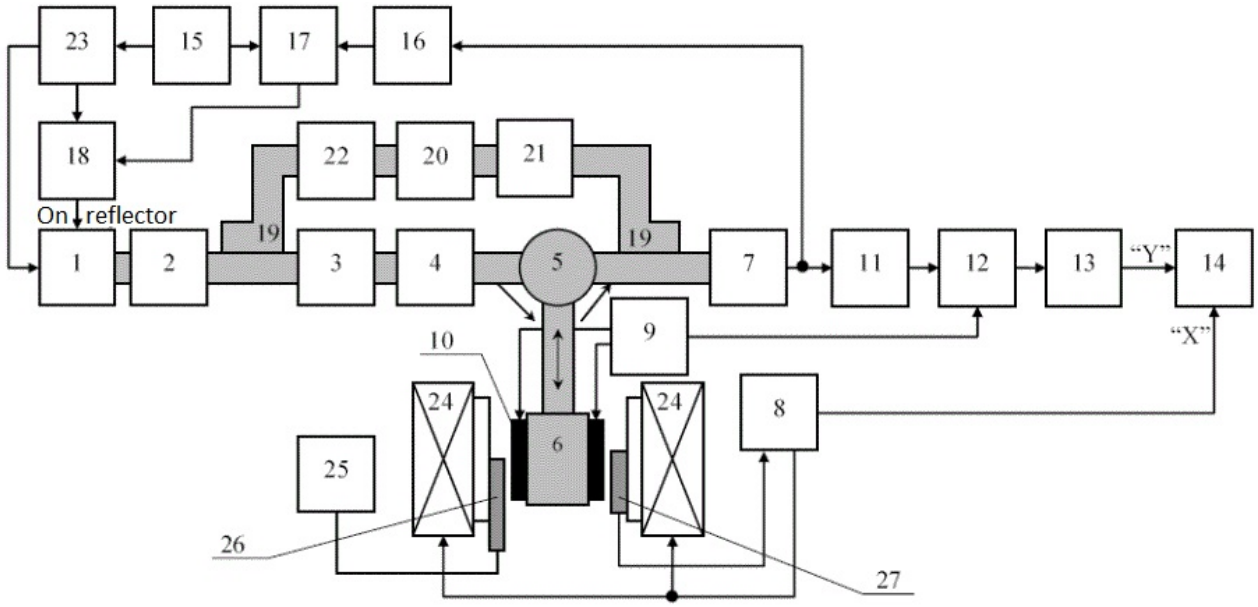

Fig. 9. Block diagram of Varian E-12 EPR spectrometer. 1 – klystron; 2 – gate; 3 – step attenuator; 4 – smoothly adjustable attenuator; 5 – circulator; 6 – resonator; 7 – microwave detector; 8 – unit for stabilization and magnetic field scan; 9 – generator of the magnetic field modulation (100 kHz); 10 – modulation coils; 11 – narrow band amplifier of EPR signal; 12 – synchronous detector of EPR signal; 13 – filter; 14 – X-Y recorder; 15 – transmission line of automatic frequency control (AFC) generator (70 kHz); 16 – narrow band amplifier of AFC transmission line (70 kHz); 17 – synchronous detector of AFC transmission line; 18 – voltage summator; 19 – directional coupler (directional-phase shifter); 20 – adjustable attenuator; 21 – variable phase shifter; 22 – bypass microwave transmission line switch; 23 – power unit of klystron; 24 – windings of magnet; 25 – magnetic gaussmeter with detecting element; 26, 27 – Hall probe of the magnetic field stabilization system.

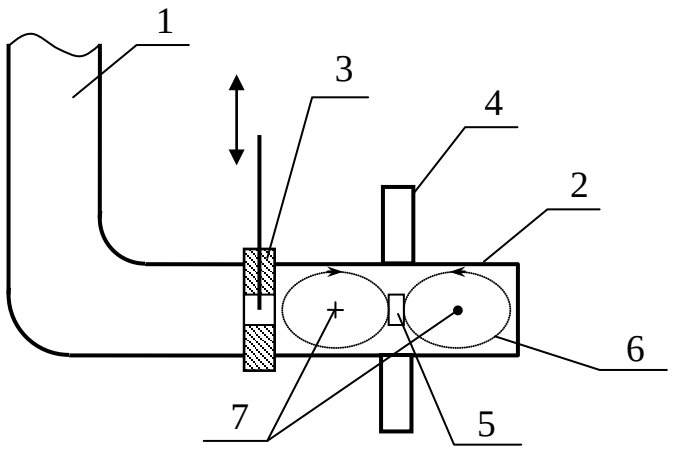

Fig. 10. The rectangular resonator with oscillations of the type H_{102} of Varian E-12 spectrometer. 1 – rectangular wave guide; 2 –resonator; 3 – coupling iris of a wave guide with the resonator which hole dimension can be changed; 4 – branch pipe for test sample 5 input into the resonator; 6, 7 – magnetic and electric field lines of a resonator.

The test sample is placed in the antinode of the magnetic component of the electromagnetic field of the resonator which is introduced into the resonator via the reach-through hole in a narrow wall of the resonator. The schematic setup of the resonator and a pattern of the field lines of magnetic and electrical components of electromagnetic field in it are shown in Fig. 10. At resonance conditions the sample starts to absorb the microwave field power that leads to change of properties of the resonator and, as consequence, to change of the power reflected from it. This change is registered in the form of EPR spectrum of the test sample.

For observation of the spectroscopic lines change slowly the magnetic field by the power supply, stabilization and field scan unit (8) near the resonant value H_0 with the amplitude larger than the absorption line width. At the moment when the field passes through the resonant value H_0 there is microwave energy absorption by the paramagnetic sample which is registered by the microwave detector - the microwave energy receiver. This is illustrated in Fig.11 which shows the magnetic field scan and a view of microwave power curve on the microwave detector in the absence and in the presence of the sample in the resonator.

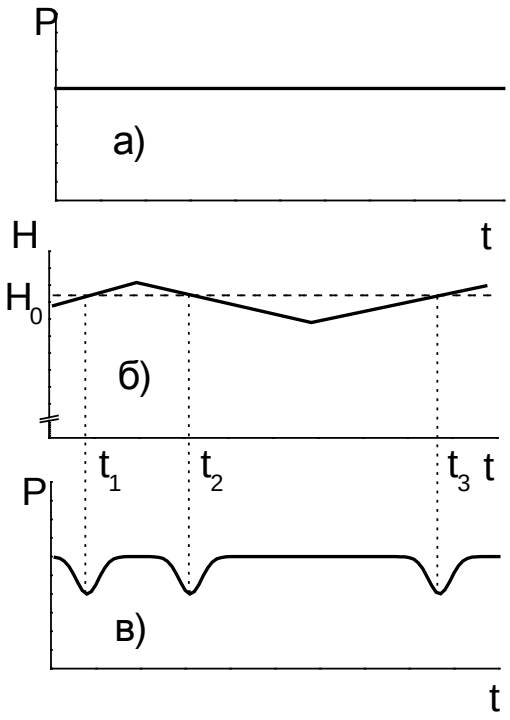

Fig. 11. Power curves of the microwave field on the microwave detector in the absence of the sample in the resonator (curve a) and in the presence of the sample in the resonator (curve b).

The absolute value of power absorbed by the sample is very small and only slightly exceeds a noise level. To amplify the signal-to-noise ratio in the device a method of double modulation of a magnetic field (the first modulation - sweep) is used. The essence of the double modulation method is as follows: slowly changing magnetic field is modulated by the high-frequency field with frequency 100 kHz (the generator (9) in Fig. 9) and with amplitude that is several times smaller compared with the absorption line half-width. For recording the very narrow lines the spectrometer is provided with possibility to use the lower modulation frequencies: 10 kHz, 1 kHz, 270 Hz, or 35 Hz.

Two coils (10) glued to wide walls of the resonator are used as the modulating device. The walls thickness in the location of coils is reduced to the value less than the thickness of a skin layer for frequency 100 kHz (approximately to 0.05 mm) so that the modulating field penetrate better through the metal walls of the resonator. If

the slowly changing magnetic field has the value far from the resonant value, a voltage on the microwave detector does not change. When approaching the resonance the absorption of microwave power by a paramagnet increases, and since the value of the magnetic field changes within the small limits with frequency of 100 kHz, the

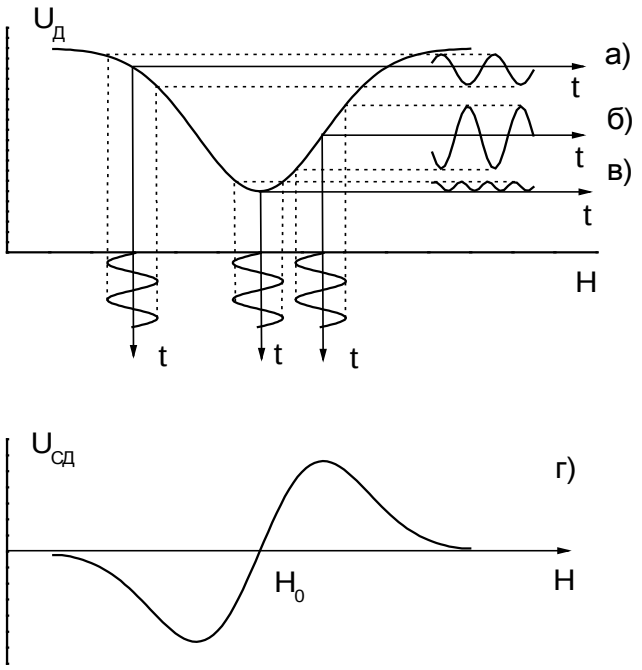

Fig. 12. A signal on the microwave detector output at "small" modulation of the magnetic field on wings (a, b) and at the center (c) of EPR lines. The output voltage of the synchronous detector *versus* the magnetic field when crossing the EPR line.

microwave power, incident on the microwave detector, i.e. and the detector current, with the same frequency starts to change. Fig. 12 shows that the alternating-current amplitude with frequency of 100 kHz on the microwave detector output at constant modulation amplitude of the magnetic field is the larger the greater is the slope of the EPR line at the given field value H, and the alternating current phase differs on 180^o on opposite wings of the line (Fig. 12 a,b). If the magnetic field has the value H_0 (adjusted precisely on center of the EPR line), there appears a signal of small amplitude with the doubled modulation frequency on the microwave detector and a signal with frequency 100 kHz is absent (Fig. 12).

Thus, application of "small" modulation of the magnetic field allows to use amplification of EPR signal after the microwave detector in the narrow frequency

range ($\Delta f \approx 10$ kHz) at modulation frequency (100 kHz) by means of narrowband amplifier (11) that essentially reduces the voltage of noise at output of registering system that have "white" spectrum and increases a signal-to-noise ratio, i.e. sensitivity of a spectrometer.

After the narrowband amplifier the EPR signal is rectified by the synchronous detector (12) which output voltage is proportional to the input voltage amplitude and the sign of the output voltage depends on the input voltage phase in respect to a reference voltage. Figure 12 shows the output voltage of the synchronous detector *versus* the magnetic field intensity. At the modulation amplitude of the magnetic field, much smaller the EPR line width, the voltage at output of the synchronous detector is close to derivative of the absorption line.

Having transited the synchronous detector with the reference frequency 100 kHz the signal after the additional filtration comes on two-coordinate recording potentiometer (14). The horizontal sweep of a recorder is synchronized with slow saw-toothed field scan. The scan time can be changed from 30 seconds to 16 hours, the sweep amplitude – from 0.2 to 10000 Oe. When recording the signals on a recorder the additional noise suppression by means of RC - filters (13) with time constant from 0.3 to 100 s is provided that raises the sensitivity of the device.

For normal operation of the radio spectrometer it is necessary that frequency of the klystron generator and the working resonator are precisely coincided. For elimination of their possible mismatch the automatic frequency control (AFC) scheme of a klystron on resonance frequency of the working resonator is used. The principle of operation of the regulating system uses the possibility of frequency change of a klystron by voltage change on its reflector.

The frequency control is carried out as follows. Apply additional voltage with small amplitude and with frequency 70 kHz on a klystron reflector from the AFC generator path (15) owing to that the frequency of a klystron appears to be modulated. If the klystron carrier frequency does not coincide with intrinsic frequency of the resonator, it appears that the microwave power reflected from the

resonator is modulated and consequently, and also the voltage on the microwave detector. The amplitude and phase of this modulation are determined by the value and sign of mismatch, i.e. the difference of the klystron frequency from the intrinsic frequency of the resonator, therefore the voltage component at the output of the microwave detector with frequency of 70 kHz can be used for stabilization of the klystron frequency, having amplified with the amplifier (16) and synchronously detected with the detector (17). The regulating voltage from the synchronous detector is applied on a klystron reflector through the summator (18) and polarity of the connection is selected in such manner as to compensate the frequency drift of a klystron from frequency of the working resonator.

If there is a necessity to carry out the EPR spectra measurements at very small microwave power (for example, in samples with long times of spin-lattice relaxation), it may appear that the microwave power reflected from the resonator is not enough to bring the microwave detector to the linear mode (to the linear sector of its current-voltage characteristic). At low power of the signal reflected from the resonator the AFC system can cease to work. In this case the bypass microwave path is used. By means of the directional coupler (19) a small portion of microwave power is tapped from the basic path through the regulated attenuator (5) and the phase transformer (21) directly on the microwave diode, bypassing a path in which the resonator is included, containing the sample in which EPR is observed. If not necessary, this bypass path can be disconnected by the cutout switch (22).

Except recording the EPR spectra with a recorder, the spectrometer has the home-made automated control and data collecting systems which allows to control the magnetic field scan and to record the spectrum in a digital form directly into the computer memory. This system consists of the communication device with the built-in analog-to-digital converter and the computer with the program, operating with Windows XP.

3. Preparation of the spectrometer for operation

Open the water gate for cold water supply to the heat exchanger unit. Switch on the actuator (green button on a dashboard located on a wall near to the power unit of the magnet) of electric power supply of power units of heat exchanger and the magnet of a spectrometer, switch on the heat exchanger pump (tumbler on the heat exchanger unit). Switch on the power supply sockets of the frequency meters, computer, magnetic gaussmeter located over the magnet. Switch on the computer and the interface of the spectrometer with the computer. Check up the position of the tumblers and switches on the console of the spectrometer and the microwave unit. Their positions should be as follows:

The radio-frequency unit:

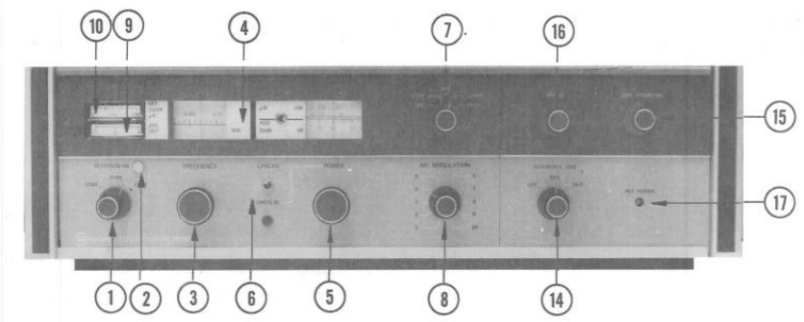

MODE switch (extreme left) shall be in STBY position;

LEVELED-UNCALIB switch – in LEVELED position;

ROWER handle– in position of not more than 0.2 mW (30 dB);

AFC switch – in NORM position;

AFC MODULATION switch – in position 5-7;

REFERENCE ARM – in ABS position;

PHASE – in midposition.

Console**:**

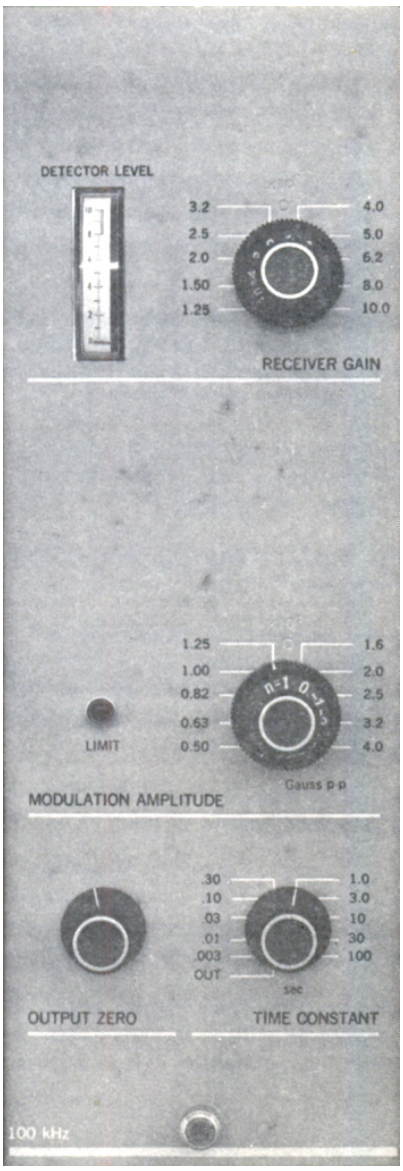

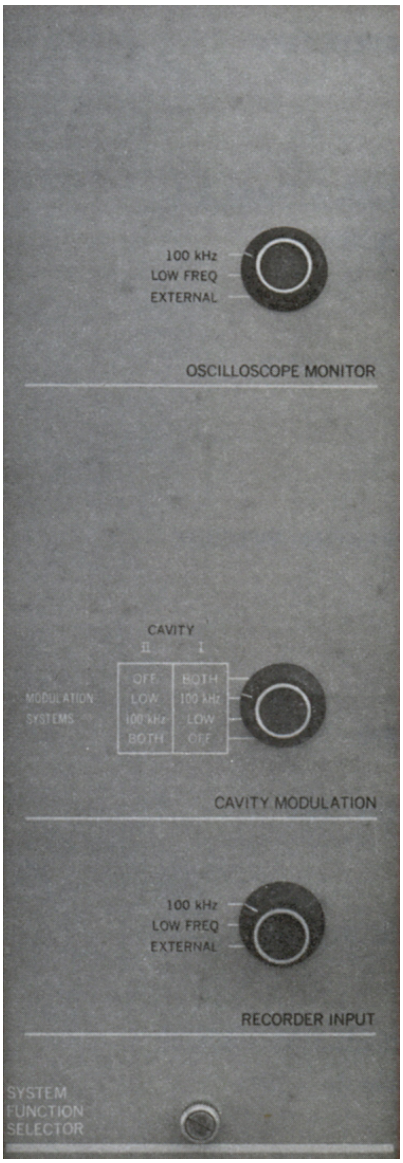

The module of receiver and modulation (100 kHz):

RECIEVER GAIN (amplification of receiver) – in position 10 x 100;

MODULATION AMPLITUDE – in position 2 Gauss p-p;

OUTPUT ZERO – in midposition;

TIME CONSTANT – in position 0.30.

SYSTEM FUNCTION SELECTOR:

CAVITY MODULATION (resonator) – in position I 100 kHz;
RECORDER INPUT – in position 100 kHz.

FIELD CONTROLLER

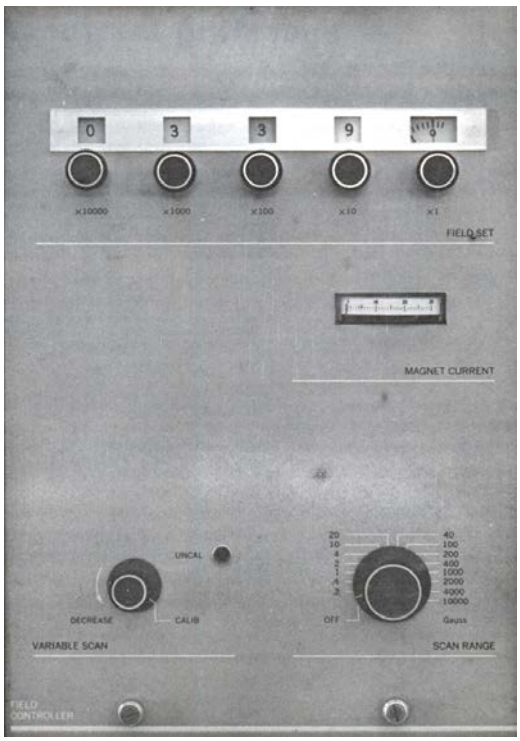

FIELD SET - 03300 G;
VARIABLE SCAN – in position CALIB (UNCAL lamp is switched off);
SCAN RANGE – in position 1000 Gauss

4. Operation procedure with a spectrometer

Switch on the console power (the switch is at the left below on the console).

MODE switch (extreme left, microwave unit) turn to TUNE position, the indicator flickers, the unit is turned on in 30 s (this delay is provided for klystron warming up).

REFERENCE ARM – switch to OFF position. The klystron generation band is observed on the oscilloscope (Fig. 13a).

Find and adjust the resonance dip at center of the generation zone band with FREQUENCY handle (Fig. 13b).

Achieve the maximum resonance dip by adjustment of matching device over the resonator, up to a base line of the generation band.

Turn the REFERENCE ARM to ON (ABS) position. Achieve the symmetrical resonance in the generation band by rotating REFERENCE ARM RHASE (Fig. 13d). Turn REFERENCE ARM to OFF position.

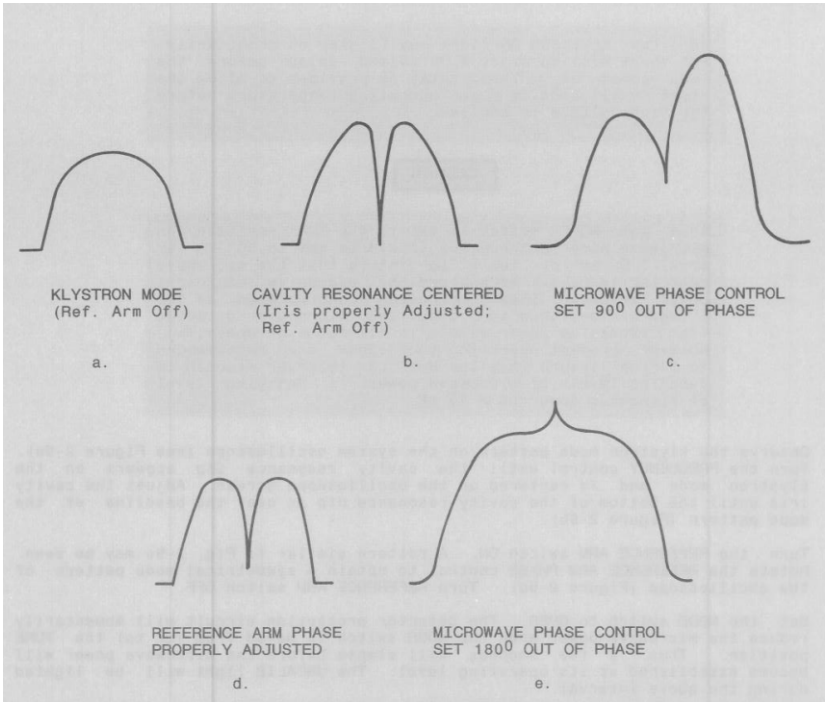

Fig. 13. Procedure for
adjustment of the resonator.

Turn MODE switch (extreme left, microwave unit) to OPERATE position.

AFC OUT indicator shall be in the middle of the scale (near to zero), showing that AFC (automatic frequency control) operates. If not, then achieve the indicator position nearby zero with handle FREQUENCY. If it is impossible or AFC OUT indicator does not responding, it is necessary to return to TUNE position and to check up a band and a dip.

If the indicator works well it is necessary to gradually increase the power by ATTENUATION handle (reducing the attenuator index towards 0 dB), simultaneously setting the adjustment of the resonator connection and achieving that

the current indicator DET CURR is around zero. After that return ATTENUATION handle position back on 30 dB.

Turn REFERENCE ARM to ON position. DET CURR indicator shall be between 150 and 300 μA.

Important! DO NOT set POWER LEVELER in OFF position when REFERENCE ARM is in ON position.

By adjusting REFERENCE ARM PHASE achieve the maximum current on DET CURR current indicator.

Reduce attenuation by ATTENUATION handle from 30 dB towards 0. At that the current of DET CURR index shall remain constant within the whole power band. If the current changes then adjust ATTENUATION on 40 or 50 dB. Record the value of a current at this level then reduce ATTENUATION down to a minimum, simultaneously maintaining the value of the recorded current value by small adjustment of the resonator connection.

Adjust with handle AFC MODULATION the minimal noise level on the oscilloscope or on the output indicator 100 kHz of RECIEVER LEVEL unit. If necessary increase the amplification RECIEVER GAIN on the unit 100 kHz. The optimum position of AFC MODULATION handle depends on the microwave power level hitting into the resonator.

Measurements of spectra

After engaging and adjustment of spectrometer it is necessary to measure the klystron frequency. The frequency of a microwave signal is divided on 1000 by Hewlett-Packard HP5260A divider and measured by frequency meter SEYFFER GR1192-B. After that start the program on the computer for measuring the EPR spectrum (double click on VarianPrim icon on a desktop). The program window is shown in Fig. 14.

The main area of the program window is filled by graphic presentation of the measured spectrum. A small yellow square on the top of this field shows the running

number of the measured spectrum point. The running intensity in mV is shown in a small yellow square on the right. The position of this small square along Y-axis corresponds to the running positions of the measured point along Y-axis of the spectrum plot.

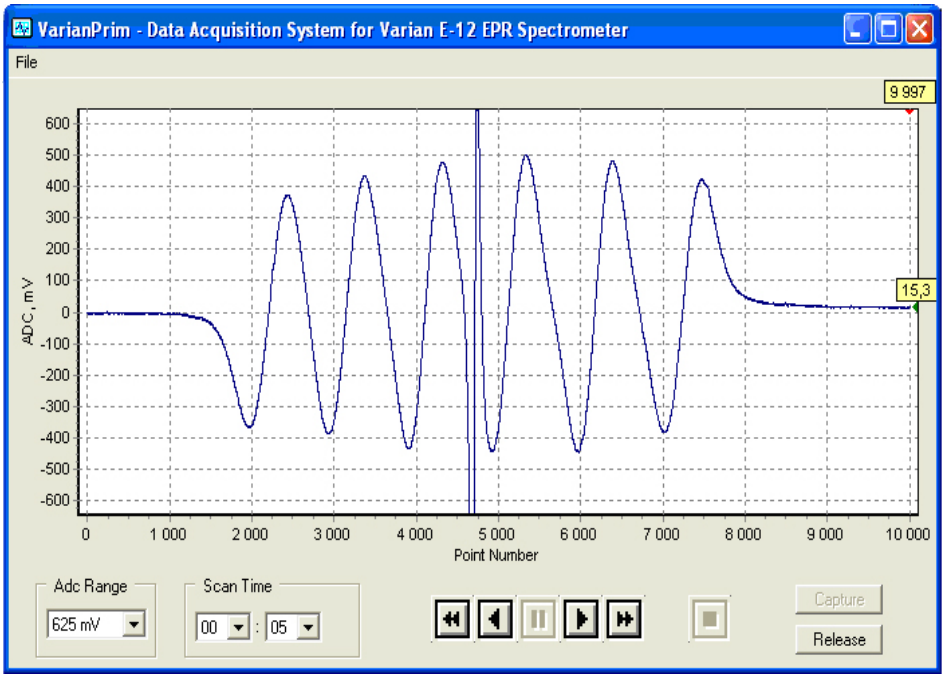

Fig. 14. Window of program for EPR spectrum recording.

- Set the following parameters of communication and control device:
  ADC range – 625 mV
  Scan Time – 00:05 (5 minutes)
- Click on Capture button. The system will automatically set the magnetic field in extreme left (low field) position of the set scan range.
- Start of measurement is carried out by pressing the button ►. The button ◄ starts spectrum recording in the opposite direction. Buttons with double triangles allow fast rewind. The button ❚❚ allows to pause temporarily the spectrum record. The termination of spectrum record is carried out by the button ■.

At first it is necessary to make a trial record of spectrum for selection of the amplification constant (RECIEVER GAIN). After that it is necessary to rewind the index of running point of the spectrum to extreme left position and start the measurement. At the beginning of recording it is necessary to pause the record (❚❚ button), measure the value of the magnetic field by means of magnetic gaussmeter ИИ1-1 and frequency meter Ч3-34, record this value and the corresponding point number of the spectrum in the logbook. After that continue record of the spectrum by pressing the ► button. Near to the right end of the spectrum repeat the measuring procedure of the magnetic field value.

After finishing of spectrum record it is necessary to record the digital data using the menu File-> Save.

To turn the spectrometer to the reset state (record mode) it is necessary to press the Release button.

Shutdown

Move the power adjustment handle ATTENUATION in MIN (60 dB) position.
MODE switch in STANDBY position.
Switch off the console power.
Switch off the heat exchanger, shut off the water.
Switch off the power.

5. Measurement of the magnetic field value

The magnetic field measurement is carried out by means of the magnetic gaussmeter ИИ1-1, allowing the measurements with accuracy up to few hundredth parts of per cent at field inhomogeneity not exceeding 0.02% per 1 cm. The measuring limits - from 250 to 25000 Oe.

Operation principle of the magnetic inductometer ІІІ1-1

The operation principle of the magnetic gaussmeter "ІІІ1-1" is based on the phenomenon of nuclear magnetic resonance (NMR). If the diamagnetic substance with the paramagnetic nuclei (with the nuclei having the magnetic dipole moments) is placed in the static magnetic field with the value H, the dipoles will start to precess around the applied field direction. The precession frequency is given by the Larmor equation:

$$\omega = \gamma H$$

where ω - cyclic frequency of precession, γ - gyromagnetic ratio of the nucleus.

To detect a precession of the magnetic dipoles the substance is placed in the inductance coil of the sensor which is a part of LC-tank of the high frequency generator. Change smoothly the frequency of the generator. When the frequency of the generator becomes equal to the precession frequency of the nuclei, there is the resonance phenomenon, i.e. energy absorption of the high-frequency magnetic field by nuclei of the working substance. This energy absorption, equivalent to reduction of a LC-tank Q-factor and, hence, equivalent to resistance of the generator circuit, causes the amplitude reduction of the generated oscillations. The generator works in the small oscillations mode at which the largest sensitivity to reduction of a Q-factor of the high-frequency coil of the sensor at the moment of NMR is provided. The magnetic field modulation by alternating current with frequency of 50 Hz with the help of the modulation coil of the sensor is provided owing to the NMR requirements are repeated twice during the modulation period.

At periodical change of the magnetic field intensity near the resonant value the amplitude change of the generated oscillations is converted after detection into the alternating current signal - NMR signal. Record the NMR signal and measure the frequency of the generator, find the magnetic field value from the equation:

$$H = C \cdot f$$

where f - frequency of the generator, C - constant of the measuring sensor. The sensor uses the NMR of hydrogen (protons) for which C = 0.234874 Oe/kHz.

Preparation for measurements

1. Set the toggle switch "Power (Сеть)" in the position "Power On (Вкл)", at that the indicator shall light up. Warm up the device for 15 minutes.

2. Press the button “Beam centering (Центровка луча)”, then set the beam at the mark on screen center with the rotary knob “Beam centering (Центровка луча)”.

3. Set the rotary knob "Frequency (Частота)" on a mark corresponding to the measured induction, for that use the approximate calibration curves placed on the front panel of the device. At measurements the sensor 3 is used, the handle "Feedback coupling (Обратная связь)“ is set in position III.

4. Set a voltage of the generated oscillations within the limits corresponding to 4-10 μA on a pointer indicator. Set the rotary knob "Amplification (Усиление)" so that the oscilloscope screen will show the device noise.

5. Set the switch “Level control (Контроль уровня)” in position “Modulation (Модуляция)”. Set the current of modulation corresponding to 4-10 μA with a pointer indicator by the rotary knob “Modulation (Модуляция)”.

Measurements operation

1. Place the sensor in the magnetic field. By slowly rotating the rotary knob "Frequency (Частота)" achieve appearance of the NMR signal on the screen (Fig. 15). Decrease the modulation current to the minimum possible value at which the NMR signal is clearly observed on the oscilloscope screen with the rotary knob “Modulation (Модуляция)”.

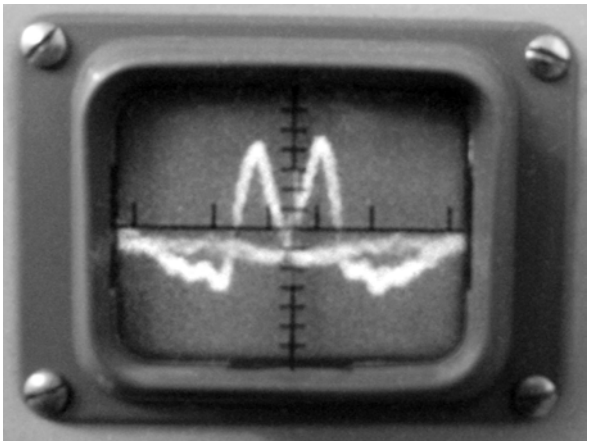

Fig. 15. NMR signal on the screen of the magnetic inductometer ИИ1-1.

2. Achieve intersection of the resonance curves with the rotary knob "Phase (Фаза)". Match the intersection point of the resonance curves with the mark in the screen center with the rotary knob "Frequency (Частота)". This adjustment corresponds to occurrence of the NMR signal at current passage in the modulation coil through zero values, and the generator frequency in this case precisely corresponds to the requirement $H = Cf$ (NMR requirement), where H – the value of the measured magnetic field.

3. Measure the device generator frequency with a frequency meter and determine the magnetic field intensity.

CALCULATION PROCEDURE FOR SPIN HAMILTONIAN CONSTANTS OF THE Mn^{2+} ION IN CaF_2 CRYSTAL

The crystal CaF_2 (fluorite) belongs to the cubic crystal system and has face-centered space lattice (space group O_h^5). Each Ca^{2+} ion (or isomorphically substituting it Mn^{2+} ion) is located at center of the cube which vertexes are filled by the fluorine ions. In a lattice in the direction of the fourfold axis these cubes are alternated with cubes in which center the cation is absent, and the cations nearest to the given cation are located in the center of the twofold axis of the same cubes.

According to high symmetry of the nearest environment the Mn^{2+} EPR spectrum in fluorite has no fine structure, consists of six lines of the hyperfine structure (Fig. 16) and is described by the following spin Hamiltonian (the axis *z* coincides with the static magnetic field direction):

$$H=g\beta HS_z+A'(S_xI_x+S_yI_y+S_zI_z).$$

The first term describes interaction with the external magnetic field (Zeeman splitting), the second one - interaction with the magnetic moment of the nucleus (hyperfine spectrum structure).

Here g - factor of spectroscopic splitting, β - Bohr magneton, S_x, S_y, S_z - moment operators of the ion electronic shell, A' - hyperfine structure constant, I_x, I_y, I_z - moment operators of the nucleus of the ion. The values of g-factor and hyperfine interaction constant can be determined from the EPR spectrum analysis.

The observed EPR spectrum indicates that the term of the Hamiltonian that describes the hyperfine structure is small compared with the Zeeman energy. Therefore the interpretation of spectra is carried out with the assumption that the Zeeman energy is the main unperturbed part of the Hamiltonian and the hyperfine interaction is considered in the form of the perturbation *V*.

The eigenvalues of the Hamiltonian can be found as follows. Using the electronic wave functions of operator S_z we find the eigenvalues taking into account

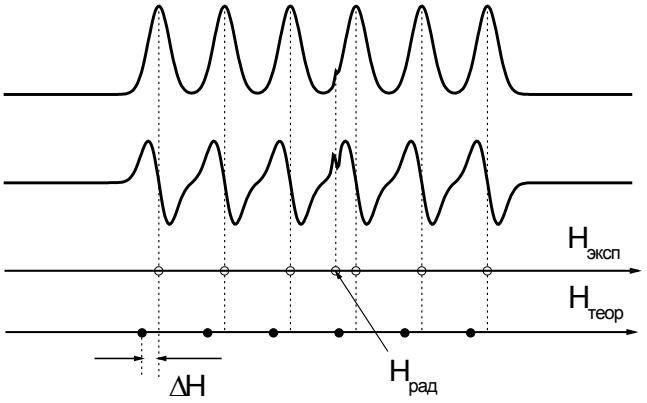

Fig. 16. EPR spectrum (primitive and derivative) of the Mn^{2+} ion in CaF_2 crystal. The EPR line of the free DPPH radical is observed near the spectrum center thus allow to measure the Mn^{2+} ion g-factor without measurement of the spectrometer frequency.

the second order of perturbation theory:

$$E_M=E_M^{(0)}+E_M^{(1)}+E_M^{(2)}=g\beta HM+\langle M|V|M\rangle+\Sigma'_M\,[(|\langle M|V|M'\rangle|^2)/(E_M^{(0)}-E_{M'}^{(0)}),$$

where $E_M^{(0)}$, $E_M^{(1)}$, $E_M^{(2)}$ – are the energy level values in the zero, first and second approximations; M and M' - magnetic quantum numbers of the electronic shell of an ion.

The resonance values of the magnetic field in which the EPR-transitions M, m – $M\pm1, m$ (m - magnetic quantum number of the nuclear moment of an ion) are observed, with accuracy up to the second approach will read as follows:

$$H_{M,\ m\ -\ M\pm1,\ m}=H_0-A\cdot m-(A^2/2H_0)\cdot[35/4-m^2-m\cdot(2M-1)].$$

Here $H_0=(h\nu/g\beta)$, where ν - measuring frequency and the hyperfine interaction constant A is expressed in $g\beta$ units ($A=A'/(g\beta)$) and is measured in Oersted.

It is better to determine the Hamiltonian constants according to the following scheme. If we write the values of fields for each value of the quantum number of the nuclear moment *m* we will obtain the following equations:

$$H_{M,\,5/2\,-\,M\pm1,5/2}=H_0-(5/2)\cdot A-(A^2/2H_0)\cdot[10/4-(5/2)\cdot(2M\text{-}1)];$$
$$H_{M,\,3/2\,-\,M\pm1,3/2}=H_0-(3/2)\cdot A-(A^2/2H_0)\cdot[26/4-(3/2)\cdot(2M\text{-}1)];$$
$$H_{M,\,1/2\,-\,M\pm1,1/2}=H_0-(1/2)\cdot A-(A^2/2H_0)\cdot[34/4-(1/2)\cdot(2M\text{-}1)]; \qquad (18)$$
$$H_{M,-1/2\,-\,M\pm1,-1/2}=H_0+(1/2)\cdot A-(A^2/2H_0)\cdot[34/4+(1/2)\cdot(2M\text{-}1);]$$
$$H_{M,-3/2\,-\,M\pm1,-3/2}=H_0+(3/2)\cdot A-(A^2/2H_0)\cdot[26/4+(3/2)\cdot(2M\text{-}1);]$$
$$H_{M,-5/2\,-\,M\pm1,-5/2}=H_0+(5/2)\cdot A-(A^2/2H_0)\cdot[10/4+(5/2)\cdot(2M\text{-}1)]$$

It is easy to see that if we take differences for pairs:

$$H_{M,-m\,-\,M\pm1,-m}-H_{M,\,m\,-\,M\pm1,\,m},$$

they will be independent on corrections to within the second order of a perturbation theory, namely:

$$H_{M,-m\,-\,M\pm1,-m}-H_{M,\,m\,-\,M\pm1,\,m}=2Am.$$

Taking *m* values from +5/2 to +1/2, we obtain three relations that allow to determine the values of the hyperfine interaction constant from the experimentally measured values of the resonance fields:

$$H_{M,-5/2\,-\,M\pm1,-5/2}-H_{M,\,5/2\,-\,M\pm1,5/2}=5A;$$
$$H_{M,-3/2\,-\,M\pm1,-3/2}-H_{M,\,3/2\,-\,M\pm1,3/2}=3A;$$
$$H_{M,-1/2\,-\,M\pm1,-1/2}-H_{M,\,1/2\,-\,M\pm1,1/2}=A.$$

We then obtain *A* values from each relation and taking the average.

To determine the spectroscopic splitting factor *g* it is supposed that the g-factor of the Mn^{2+} ion is equal to the g-factor of the free radical (α,α'-diphenyl-β-picrylhydrazyl) and is equal to 2.0036, and from equations (18) one calculates the theoretical positions of lines with this g-factor, taking the measured field as H_0 in which the EPR line of the free radical is observed. Taking differences of the theoretical calculations with the experimentally observed resonance values of the fields, we obtain the shift ΔH of each EPR line due to deviation of the g-factor of the Mn^{2+} ion from the g-factor of the free radical.

From the shift ΔH averaged over all lines we determine the true value of the spectroscopic splitting factor:

$$g = (g_{pad} H_{pad}) / (H_{pad} \pm \Delta H).$$

The field of radical is usually measured at experiment. The sign of ΔH is taken depending on what prevails: theoretical calculations or experiment. If the theoretical calculations give the overestimated values of the resonance fields then take the sign "-", if underestimated "+".

RESEARCH TASK

Research the EPR spectrum of the Mn^{2+} ion in CaF_2 fluorite:

1. Measure the resonance values of the static magnetic field H_{Res} for all observable EPR-transitions, including the EPR line of DPPH radical;

2. Calculate the constants g and A of the spin Hamiltonian.

WORK PROCEDURE

1. Study the EPR theory, procedure of experiment and experimental technique, description of the devices used in installation.

2. Pass the test according to section 1 and obtain the permit-to-experiment.

3. Perform the experimental research of the EPR spectra.

4. Perform the calculations specified in the research task.

5. Pass the test according to sections 3 and 4.

Authors are grateful to the associate professor of quantum electronics and radiospectroscopy department V.G. Stepanov whose methodical textbooks formed the basis of the present practical work.

References

1. S.V. Vonsovsky, Magnetism of microparticles. Moscow, Nauka, 1973 [in Russian].

2. S.A.Altshuler, B.M.Kozyrev. Electron paramagnetic resonance of compounds of the intermediate group of elements. Moscow, Nauka, 1972 [in Russian].

3. Poole, C. Electron Spin Resonance a Comprehensive Treatise on Experimental Techniques, Editions 1, 2: Interscience Publishers, New York, (1967), (1983).

4. V.M. Vinokurov, M.M. Zaripov, V.G. Stepanov. A study of some Mn-containing carbonates by the method of electron paramagnetic resonance. Sov. Phys. Crystallogr. v. **6**, pp.83-86, 1961.

5. Varian E-12 EPR Radio spectrometer. Technical specification and operation manual.

6. Magnetic field intensity meter ИИ1-1. Technical specification and operation manual [in Russian].

PART 2

1. Basics of EPR theory of rare-earth ions in ionic crystals

1.1. Free ions

The family of the rare earth ions or lanthanides forms a special group of the elements which chemical properties are very similar. Their valence is usually equal to three. The closed electronic shells correspond to the atomic core of xenon:

$$1s^2\ 2s^2\ 2p^6\ 3s^2\ 3p^6\ 3d^{10}\ 4s^2\ 4p^6\ 4d^{10}\ 5s^2\ 5p^6;$$

the La^{3+} ion is in this state. In the subsequent ions the electrons gradually fill a 4f-shell; the Lu^{3+} ion has the filled 4f-shell. Table 1.1 shows the basic characteristics of triple-charged ions.

Outside of the atomic core of a xenon the electrons have a configuration $4f^{n}$, where n = Z – 57 and Z – atomic number of lantanide. In almost all cases the magnetic properties of ions are determined by the number of electrons in a 4f-shell. The coupling of electrons is close to *LS*-type (Russell-Saunders coupling), at that the ground state of the ion is determined by the Hund's rule. The total moment of gyration (angular moment) is described by the quantum number $J = L + S$ (**L** and **S** – are the orbital and spin moments) and the corresponding value of Lande splitting factor (g-factor):

$$g_J = \frac{3}{2} - \frac{L(L+1) - S(S+1)}{2J(J+1)}. \qquad (1)$$

The resulting electronic magnetic dipole moment is equal to:

$$\boldsymbol{\mu}_J = -g_J \mu_B \mathbf{J}, \qquad (2)$$

where $\mu_B = e\hbar/2mc$ – Bohr magneton. Equation (2) is valid while it is possible to neglect all interactions which mix the states with different *J*.

The Hamiltonian of spin-orbit interaction $\xi(\mathbf{l}\,\mathbf{s})$ in *LS* – coupling approach may be written as follows:

$$H_{SO} = \lambda\ (\mathbf{LS}). \tag{3}$$

For the basic terms obeying the Hund's rule (i.e. the terms with the maximum spin *S*), $\lambda = \pm(\xi/2S)$. Plus and minus signs correspond to the electronic shells that are less or more than half filled, respectively. The spin-orbit interaction splits the given term on a multiplet of levels with different values of the full angular moment *J*.

The energy of level *J* is determined by the equation:

$$\mathrm{E}_J = \frac{1}{2}\lambda\left\{J\left(J+1\right) - L\left(L+1\right) - S\left(S+1\right)\right\}, \tag{4}$$

from which the Lande intervals rule is as follows:

$$\mathrm{E}_J - \mathrm{E}_{J-1} = \lambda\ J. \tag{5}$$

Experimentally these intervals are determined from the optical absorption and luminescence spectra.

Table 1.1

Element	Atomic number Z	Ion	Electron confi-guration	Ground state	Lande splitting factor g_J	Excited state	Energy of excited state, cm^{-1}
Lanthanum	57	La^{3+}	$4f^0$				
Cerium	58	Ce^{3+}	$4f^1$	$^2F_{5/2}$	6/7	$^2F_{7/2}$	2200
Praseodymium	59	Pr^{3+}	$4f^2$	$^3H_4$	4/5	$^3H_5$	2100
Neodymium	60	Nd^{3+}	$4f^3$	$^4I_{9/2}$	8/11	$^4I_{11/2}$	1900
Promethium	61	Pm^{3+}	$4f^4$	$^5I_4$	3/5	$^5I_5$	1600
Samarium	62	Sm^{3+}	$4f^5$	$^6H_{5/2}$	2/7	$^6H_{7/2}$	1000
Europium	63	Eu^{3+}	$4f^6$	$^7F_0$	0	$^7F_1$	400
Gadolinium	64	Gd^{3+}	$4f^7$	$^8S_{7/2}$	2	$^6P_{7/2}$	30000
Terbium	65	Tb^{3+}	$4f^8$	$^7F_6$	3/2	$^7F_5$	2000
Dysprosium	66	Dy^{3+}	$4f^9$	$^6H_{15/2}$	4/3	$^6H_{13/2}$	3400
Holmium	67	Ho^{3+}	$4f^{10}$	$^5I_8$	5/4	$^5I_7$	5000
Erbium	68	Er^{3+}	$4f^{11}$	$^4I_{15/2}$	6/5	$^4I_{13/2}$	6500
Thulium	69	Tm^{3+}	$4f^{12}$	$^3H_6$	7/6	$^3H_5$	8200
Ytterbium	70	Yb^{3+}	$4f^{13}$	$^2F7/2$	8/7	$^2F_{5/2}$	10000
Lutetium	71	Lu^{3+}	$4f^{14}$				

1.2. Lanthanide compounds

The lanthanide ions enter into many chemical compounds, but we will restrict ourselves to discussion of only several types of compounds, in which the local symmetry is not reduced to below the axial one and in which a series of the Ln^{3+} ions has been studied.

The first compounds of these type are ethylsulphates of lanthanides $Ln(C_2H_5SO_4)_3 \cdot 9H_2O$. The space symmetry group of ethylsulphates is $P6_3/m$, a point symmetry group of the Ln^{3+} ion environment – C_{3h}. This ion has nine molecules of water as the nearest neighbors: six of them form a triangular prism, at that three molecules are located above, and three – below the mirror plane containing three remained water molecules and Ln^{3+} ion. In water molecules the oxygen atoms are the nearest to the rare-earth ion; in erbium ethylsulphate, for example, the distances from the Er^{3+} ion to the six O^{2-} ions forming a prism, are equal to 2.37 Å, and the distances to three O^{2-} atoms, lying in the symmetry plane, – 2.52 Å. The symmetry of the nearest environment of the Ln^{3+} ion is close to D_{3h} (the symmetry elements of group D_{3h} – vertical triad axis, horizontal plane and three vertical symmetry planes).

The second group of compounds very similar with ethylsulphates from EPR results, form anhydrous trichlorides of type $LaCl_3$ which crystallize in structure with space symmetry $C6_3/m$; the point symmetry of environment of ion is C_{3h}. The nearest neighbors of the La^{3+} ion are the nine approximately equidistant Cl^- ions. Three ions of chlorine lie in one plane with La^{3+} at a distance of 2.97 Å from it. Six other ions are located at a distance of 2.99 Å from the La^{3+} ion, at that three of them lie above in the parallel plane, and three - in the parallel plane below La^{3+}. All rare-earth ions introduced into $LaCl_3$ as an impurity do not change the structure of this compound, but the major part of undiluted trichlorides with the heavier ions have different structure (orthorhombic), similar to that of YCl_3.

The third group with a bit different symmetry are formed by a nitrates of the type $Ln_2Mg_3(NO_3)_{12} \cdot 24H_2O$. These are the rhombohedric crystals with the space group $R\bar{3}$. The Ln^{3+} ion is surrounded by twelve atoms of oxygen with the distances to which are 2.64 Å in average; These atoms belonging to $(NO_3)^-$ are located in the corners of the distorted icosahedron. Research of optical spectra and EPR confirmed that the crystal electric field has symmetry close to icosahedral. The point symmetry group of the Ln^{3+} (Ln = La, Ce, Pr, Nd) ion environment are close to C_3, but in general the optical spectroscopy and magnetic resonance data were interpreted with

C_{3v} symmetry. The nitrates are remarkable in the sense that the rare-earth ions in them are separated by large distances, e.g. in cerium-magnesium the nearest Ce^{3+} ions are located at a distance of 8.56 Å. Due to strong natural dilution the nitrates (especially cerium-magnesium) are used in ultralow temperature equipment – as paramagnetic salts in the adiabatic demagnetization refrigerators and thermometric compounds. Ethylsulphates of lanthanides are also magnetically diluted, the nearest Ln^{3+} ions in them are separated by the distance of 7.1 Å (along the *c* axis). In trichlorides the nearest rare-earth ions are also located along the *c* axis but the distance between them is much smaller – 4.3 Å.

The fourth group of compounds is formed by tetrafluorides of lanthanides $LiLnF_4$ (Ln = Tb, Dy, Ho, Er, Tm, Yb and Y). They have tetragonal structure of scheelite ($CaWO_4$), space symmetry group $I4_1/a$. The point symmetry group of the Ln^{3+} ion is S_4; the lanthanide ion fills two positions in a unit cell, but these positions are related by (001) plane reflection and are therefore the magnetically equivalent. The nearest environment of the Ln^{3+} ion consists of the eight F^- ions at the distance of 2.3 Å, while the lithium ion has the tetrahedral environment with tetragonal distortion.

The fifth group of crystals consists of phosphates, arsenates and vanadates of lanthanides $LnBO_4$ (B = P, As, V). At room temperature these crystals have tetragonal zirconium structure ($ZrSiO_4$), space symmetry group $I4_1/amd$. The point symmetry of the Ln^{3+} ion environment – D_{2d}, the nearest environment is the four O^{2-} ions at a distance of 2.3 Å.

Finally, the sixth group is the crystals with cubic structure of elpasolite. Their joint formula – A_2BLnCl_6, space symmetry group (at room temperature) – F*m*3*m*, the point symmetry of the Ln^{3+} ion environment (also for univalent ions A^+ and B^+) – cubic. The Ln^{3+} ions are located in the sites of face-centered cubic (fcc) lattice, the distance between them is approximately 7 Å. Each lanthanide ion is in the center of regular octahedron of the Cl^- ions, the same environment has the B^+ ion. The A^+ ion is

located in the center of cube at that the four B^+ ions and the four Ln^{3+} ions are located in this cube sites, and Cl^- is in the center of each facet.

In many cases the lanthanide ions may be implanted in the foreign compounds instead of the bivalent metal ions like cadmium, calcium, lead, magnesium, etc. For example CdF_2, CaF_2, SrF_2, PbF_2 and BaF_2 may be doped by Ln^{3+}. These crystals have cubic symmetry, their lattice parameters are equal to 5.40 Å, 5.45 Å, 5.86 Å, 5.93 Å and 6.19 Å, respectively. The CaF_2 structure may be considered as simple sequence of cubes formed by the F^- ions with the Ca^{2+} ions located in the center of every second cube. Thus the calcium ion is located in the center of a cube formed by eight fluorine ions, the Ca-F distance is 2.36 Å. The rare-earth ion replace calcium, however the symmetry of their environment is not always the cubic one. If the nearest vacant interstitial site (center of the neighboring cube) is occupied by the excess F^- ion, then there is a tetragonal symmetry. The trigonal symmetry of the Ln^{3+} center is realized in the case when the oxygen (O^{2-}) ion replaces the F^- ions in one of the cube vertex. The paramagnetic La^{3+} centers with cubic symmetry are observed when compensation of the electric charge is not nearby the rare-earth ion, but at the remote sites. It shall be noted that crystals of the type CaF_2, $CaWO_4$, $KMgF_3$ and others, doped by the triple-charged rare-earth ions have wide application as active substances of the optic quantum amplifiers and generators (lasers).

1.3. Crystal electric field

We will take into account the interaction approximately between the free ions in a crystal, considering that each ion is in some electric field created by all surrounding particles. This field we will call the crystal field. The idea about the crystal field put forward by Becquerel, thanks to works of Bethe, Kramers, Van-Fleck, Elliott and Stevens, transformed into the well-developed theory and allowed to

explain the diverse physical and chemical properties of compounds with transition group elements.

A crystal field effect is always weaker compared with Coulomb interaction between electrons in atom. Therefore we can use a self-consistent field method and to consider the configuration of electrons forming an open shell of a paramagnetic ion. The self-consistent field method does not consider completely the electrostatic interaction between the electrons. Therefore, it is necessary to know for the calculations that are usually carried out by a perturbation technique in what relation there are the missed part of a coulomb repulsion between the electrons, magnetic coupling between their spin and orbital moments and crystal field forces. The crystal field is considered as intermediate if its effect is stronger compared with the spin-orbit coupling of electrons, but is much weaker compared with interactions between the separate electrons. This case is realized in compounds of iron elements group. As to rare-earth compounds, a weak crystal field which is not able to disturb the coupling between the orbital and spin moments of all open electronic shell is acting in it.

The character of energy levels splitting of paramagnetic ions by a crystal field depends on symmetry of this field and is easily determined by means of the group theory methods. Tables 1.2a and 1.2b show the number of energy sublevels appearing in the field of the corresponding symmetry for the integer and half-integer values of quantum number *J*; the numbers in brackets denote a degeneracy of these sublevels.

Table 1.2a

J	Splitting in the crystalline field of			
	cubic symmetry	trigonal symmetry	tetragonal symmetry	rhombic symmetry
0	1 (1)	1 (1)	1 (1)	Complete

1	1 (3)	2=1 (1) +1 (2)	2=1 (1) +1 (2)	splitting
2	2=1 (2) +1 (3)	3=1 (1) +2 (2)	4=3 (1) +1 (2)	
3	3=1 (1) +2 (3)	5=3 (1) +2 (2)	5=3 (1) +2 (2)	
4	4=1 (1) +1 (2) +2 (3)	6=3 (1) +3 (2)	7=5 (1) +2 (2)	
5	4=1 (2) +3 (3)	7=3 (1) +4 (2)	8=5 (1) +3 (2)	
6	6=2 (1) +1 (2) +3 (3)	9=5 (1) +4 (2)	10=7 (1) +3 (2)	
7	6=1 (1) +1 (2) +4 (3)	10=5 (1) +5 (2)	11=7 (1) +4 (2)	
8	7=1 (1) +2 (2) +4 (3)	11=5 (1) +6 (2)	13=9 (1) +4 (2)	

From Table 1.2b we see that in the case of a half-integer spin the energy sublevels remain always at least twice degenerate. This fact is a consequence of the general Kramers theorem that has the fundamental value for the theory of paramagnetism.

The theorem says: electrical forces are not able to remove completely the degeneracy of the energy level of the system that contains the odd number of electrons.

Table 1.2b

J	Distribution in crystal field of	
	cubic symmetry	lower symmetry
1/2	1=1 (2)	1 (2)
3/2	1=1 (4)	2 (2)
5/2	2=1 (2) +1 (4)	3 (2)
7/2	3=2 (2) +1 (4)	4 (2)
9/2	3=1 (2) +2 (4)	5 (2)
11/2	4=2 (2) +2 (4)	6 (2)
13/2	5=3 (2) +2 (4)	7 (2)
15/2	5=2 (2) +3 (4)	8 (2)

This implies that the paramagnetic resonance, as a rule, can be observed on the paramagnetic ions containing the odd number of electrons since the magnetic field, removing degeneration of the basic energy level, may cause the splittings lying in the radio-frequency band. It is necessary only that the transitions between the magnetic sublevels are not forbidden. If the number of electrons is even then already in the

absence of a magnetic field all levels may be undegenerate and so far apart from each other that it is not possible to observe a paramagnetic resonance at any values of the really achievable magnetic fields.

For calculation by a perturbation technique of crystal field effect on energy levels of paramagnetic ions it is necessary to calculate first the matrix elements of energy H_{KP} of electrons of the open shell in a crystal electric field. It is possible to present the energy H_{KP} in a form

$$\mathsf{H}_{KP} = \sum_i -eV\left(x_i, y_i, z_i\right), \tag{6}$$

where V – crystal field potential, x_i, y_i, z_i – i-th electron coordinates of the open shell. Supposing that electronic shells of paramagnetic atom and particles surrounding it do not overlap with each other and that, hence, the potential V satisfies the Laplace equation, we can perform for it the spherical harmonic expansion:

$$V = \sum_{k=0}^{\infty} \sum_{q=-k}^{k} B_k^q \gamma^k Y_k^q\left(\theta,\varphi\right) = \sum V_k^q. \tag{7}$$

The signs of spherical harmonics are defined so that $Y_k^{q^*} = \left(-1\right)^q Y_k^{-q}$. The symmetry of an environment imposes some restrictions for the coefficients B_k^q. For example, in the presence of inverse center in expansion (7) the harmonics with odd k are absent; besides, owing the reality of potential it is necessary, that the following requirement is satisfied $B_k^q = \left(-1\right)^q B_k^{q^*}$.

We will be interested in not the absolute energy level shifts, but only their splitting in a crystal field. Therefore we can, without loss of generality, omit the term with $k = 0$ in expansion (7).

Now the problem is reduced to evaluation of matrix elements of a crystal field (or crystal-field potential) between the wave functions Ψ which are the Slater determinants or their linear combinations. Each determinant will be of the type $\left(\chi_1,...,\chi_N,\varphi_1,...,\varphi_P\right)$. The first N one-electron functions $\chi_1,...,\chi_N$ correspond to the filled shells; they are identical in all Slater determinants appearing in the

expansion of states Ψ of a paramagnetic ion. The other one-electron wave functions $\varphi_1, \ldots, \varphi_P$ correspond to magnetic electrons of the open shells; hence, it is the functions of the type $\left|l, m_l, m_s\right\rangle$, where $l = 2$ for d-electrons and $l = 3$ for f-electrons. The potential of a crystal field $V = \sum_i V_i$ is the sum of the one-electron operators. Accordingly, each matrix element $\left\langle \Psi \middle| V \middle| \Psi' \right\rangle$ is the sum of the one-electron matrix elements $\left\langle \Psi_a \middle| V \middle| \Psi_b \right\rangle$, where Ψ_a, Ψ_b – wave functions of electrons χ of the filled shells and functions of electrons φ of the open shells. The contribution of the filled shells to a matrix element $\left\langle \Psi \middle| V \middle| \Psi' \right\rangle$ looks like $\sum_{j=1}^{N} \left\langle \chi_j \middle| V \middle| \chi_j \right\rangle$ and is equal to zero since we have omitted the term with $k = 0$ in expansion (7). Therefore in general we cannot consider the filled shells and to write our Slater determinant in the form $\left(\varphi_1, ..., \varphi_P\right)$, i.e. to construct it of the wave functions of magnetic electrons only. Then the one-electron matrix element is written in the following form:

$$\sum_{k,q} \left\langle l, m_l, m_s \middle| V_k^q \middle| l, m_l', m_s' \right\rangle = \sum_k \left\langle r^k \right\rangle \sum_q B_k^q \left\langle l, m_l \middle| Y_k^q \middle| l, m_l' \right\rangle \delta\left(m_s, m_s'\right), \qquad (8)$$

where

$$\text{где } \left\langle r^k \right\rangle = \int_0^\infty \left| f_l(r) \right|^2 r^k r^2 dr, \qquad (9)$$

and $f_l(r)$ – radial wave function. The matrix elements of the operator V_k^q are zero if the following requirements are violated:

$$k \le l, \;\; m_l = q + m_l'. \qquad (10)$$

The selection rule $k \le l$ essentially reduces the number of the parameters necessary for description of the crystal potential. Besides, even in the absence of the symmetry center it is possible to omit the terms V_k^q with odd k since the corresponding matrix elements are equal to zero.

The number of terms of series (7) decreases only owing to symmetry of the environment. If the environment has a symmetry axis of the second order, parallel to the quantization axis, or symmetry plane, perpendicular to it, then only the terms with the even coefficient q are remained. If there is the third order axis there are only q values, multiple of three.

In the presence of a plane symmetry, perpendicular to the quantization axis of the third order (C_{3h} symmetry), the coefficients $B_k^{|q|}$ can be made real by a corresponding choice of plane xOz. In the case of C_{3h} symmetry the terms with $q \neq 0$ at $l = 2$ are absent, and at $l = 3$ there is only one term:

$$B_6^6 Y_6^6 + B_6^{-6} Y_6^{-6} = B_6^6 Y_6^6 + B_6^{6*} Y_6^{6*} = \frac{B_6^6 + B_6^{6*}}{2}\left(Y_6^6 + Y_6^{6*}\right) - \frac{B_6^6 - B_6^{6*}}{2i} \cdot \frac{Y_6^6 - Y_6^{6*}}{i};$$

by transformation of rotation around the axis z it is always possible to achieve that $B_6^6 - B_6^{6*} = 0$. The same type of considerations lead to the similar relations in case of C_{4h} or D_4 symmetry when only the terms with $|q| = 0$ and $|q| = 4$ are different from zero.

If the potential has cubic symmetry then there exists only one combination of spherical harmonics of the fourth order, invariant relative the cubic group, and only one – of the sixth order:

$$\underline{k = 4}, \quad V_4 = b_4 r^4 \left\{ \sqrt{\frac{14}{24}} Y_4^0 + \sqrt{\frac{5}{24}} \left(Y_4^4 + Y_4^{-4}\right) \right\}; \tag{11}$$

$$\underline{k = 6}, \quad V_6 = b_6 r^6 \left\{ \frac{2}{\sqrt{32}} Y_6^0 - \sqrt{\frac{14}{32}} \left(Y_6^4 + Y_6^{-4}\right) \right\}. \tag{12}$$

The coefficients b_4 and b_6 are defined so that functions V_4/b_4 and V_6/b_6 were normalized to unity on unit sphere.

Though the expansion of crystal potential of the type (7) is more natural, in the literature it is usually accepted to expand it on the homogeneous polynomials of the power k, each of them represents a certain combination of spherical harmonics,

without paying special attention on normalization of these polynomials. If symmetry is such that the coefficients B_k^q in the expansion (7) are real, then this new expansion looks as follows:

$$V = \sum_k \sum_{q>0} \mathrm{A}_k^q P_k^q(x, y, z), \tag{13}$$

where P_k^q – unnormalized homogeneous polynomials proportional to $r^k\left(Y_k^q + Y_k^{q*}\right)$ which should not be confused, however, with Legendre polynomials designated in a similar fashion. Table 1.3 shows the polynomials in the case of tetragonal, hexagonal and cubic symmetry of the crystal field, and also the relation between the coefficients A_k^q in expression (13) and B_k^q in (7).

In case of cubic symmetry the polynomials:

$$P_4 = P_4^0 + 5P_4^4 = 20\left(x^4 + y^4 + z^4 - \frac{3}{5}r^4\right), \tag{14}$$

$$\begin{aligned} P_6 = P_6^0 - 21P_6^4 = -14\cdot 16\Big\{ & x^6 + y^6 + z^6 + \frac{15}{4}\big(x^4y^2 + y^4x^2 + \\ & + x^4z^2 + z^4x^2 + y^4z^2 + z^4y^2\big) - \frac{15}{4}r^6\Big\}, \end{aligned} \tag{15}$$

are introduced and the cubic potential is written as follows:

$$V_{CUBE} = A_4P_4 + A_6P_6, \tag{16}$$

where the coefficients A_4 and A_6 are related to coefficients b_4 and b_6 in expressions (11) and (12) through the following relations:

$$A_4 = \frac{1}{\sqrt{2\pi}}\cdot\frac{3}{16}\sqrt{\frac{7}{6}}\,b_4, \quad A_6 = \frac{1}{\sqrt{2\pi}}\cdot\frac{\sqrt{13}}{64}\,b_6. \tag{17}$$

The coefficients A_4 and A_6 can be calculated in the so-called “point charge approach” by expansion of the quantity $\sum_i \frac{1}{|\mathbf{r}-\mathbf{R}_i|}$; here the vectors $\mathbf{R}_i$ determine the position of charges that create the potential. The electrostatic energy of electron with

charge $-e$ in the field of six charges $-Ze$, located in vertexes of the regular octahedron, is given by the equations (14) - (17), and

$$A_{4(OCTAHEDRON)}=\frac{7}{16}\cdot\frac{Ze^2}{R^5},\ A_{6(OCTAHEDRON)}=\frac{3}{64}\cdot\frac{Ze^2}{R^7}. \qquad (18)$$

Here R – distance of each charge $-Ze$ from octahedron center.

If the paramagnetic ion is surrounded by eight charges located in vertexes of a cube,

Table 1.3

$P_2^0=3z^2-r^2$	$P_4^4=x^4-6x^2y^2+y^4$
$P_4^0=35z^4-30z^2r^2+3r^4$	$P_6^4=\left(11z^2-r^2\right)\left(x^4-6x^2y^2+y^4\right)$
$P_6^0=231z^6-315z^4r^2+105z^2r^4-5r^6$	$P_6^6=x^6-15x^4y^2+15x^2y^4-y^6$
$A_2^0=\frac{1}{\sqrt{2\pi}}\cdot\sqrt{\frac{5}{8}}B_2^0$	$A_4^4=\frac{1}{\sqrt{2\pi}}\cdot\frac{3\sqrt{35}}{8}B_4^4$
$A_4^0=\frac{1}{\sqrt{2\pi}}\cdot\frac{3\sqrt{2}}{16}B_4^0$	$A_6^4=\frac{1}{\sqrt{2\pi}}\cdot\frac{3\sqrt{13\cdot28}}{32}B_6^4$
$A_6^0=\frac{1}{\sqrt{2\pi}}\cdot\frac{\sqrt{26}}{32}B_6^0$	$A_6^6=\frac{1}{\sqrt{2\pi}}\cdot\frac{\sqrt{13\cdot21\cdot22}}{32}B_6^6$

$$A_{4(CUBE)}=-\frac{7}{18}\cdot\frac{Ze^2}{R^5},\ A_{6(CUBE)}=\frac{1}{9}\cdot\frac{Ze^2}{R^7}, \qquad (19)$$

where R is again the distance of each charge $-Ze$ from the cube center.

1.4. Equivalent operators

Having obtained the expansions (7) or (13) for the crystal field potential we are faced with the problem of evaluation of the matrix elements $\left\langle\Psi\middle|V\middle|\Psi'\right\rangle$. The

rectilinear approach would consist in expansion of functions Ψ and Ψ′ on Slater determinants that would allow to reduce the matrix element $\langle \Psi | V | \Psi' \rangle$ to the sum of the one-electron matrix elements of the type $\langle l, m_l | V | l, m_l' \rangle \, \delta(m_s, m_s')$.

It is much more preferable to express the functions Ψ and Ψ′ via eigenstates $|L, S, J, M_J\rangle$ of operator J and to apply the Wigner-Eckart theorem. From the components J_x, J_y, J_z of vector **J** we compose the so-called "equivalent operators" – the tensor operators O_k^q possessing the same properties of transformation, as the polynominals P_k^q defined in Table 1.3. Then within each set of functions with the given J we can write the equality:

$$\left\langle J, M_J \left| \sum_i P_k^q(\mathbf{r}_i) \right| J, M_J' \right\rangle = a_k \langle r^k \rangle \left\langle J, M_J \left| O_k^q(\mathbf{J}) \right| J, M_J' \right\rangle, \qquad (20)$$

where summation $\sum_i$ is carried out with all electrons. The matrix elements $\sum P_k^q$ of the corresponding equivalent operators coincide to within some common factor, identical for all functions with equal k. Thus, the cumbersome direct calculations of the matrix elements of the crystal field potential can be replaced by simple evaluations of matrix elements of polynomials of the second, fourth and sixth degrees of J_x, J_y, J_z.

Direct calculations nevertheless are necessary for determination of common factor a_2, a_4, a_6. In the literature these factors are called the Stevens coefficients and designated, accordingly, as α, β, γ or $\langle J \| \alpha \| J \rangle, \langle J \| \beta \| J \rangle, \langle J \| \gamma \| J \rangle$. The Stevens coefficients for all rare-earth ions can be determined by means of the wave functions corresponding to the states with maximum J_z, by transition from the representation J, J_z to the representation L_z, S_z and then to the representation l_z, s_z. The values of the coefficients α, β, and γ are given in monographies [1, 2].

Construction of polynomials O_k^q is nontrivial, since the components J_x, J_y, J_z do not commute with each other. Therefore, if we find the expression $x^\lambda y^\mu z^\nu$ in a

polynomial P_k^q, in polynomial O_k^q it is replaced not by $J_x^\lambda J_y^\mu J_z^\nu$, but by a symmetrized product, i.e. by an average of every possible products in which J_x, J_y, J_z are met λ, μ, ν times, respectively. It is possible then to simplify this average, using the commutation rules of the operators J_x, J_y, J_z. In Table 1.4 we give the list of some equivalent operators O_k^q, using the designation $\{A, B\}_S = \frac{1}{2}(AB + BA)$. The matrix elements of operators O_k^q are tabulated in [1, 2].

Table 1.4

$O_2^0 = 3J_z^2 - J(J+1)$
$O_4^0 = 35J_z^4 - 30J(J+1)J_z^2 + 25J_z^2 - 6J(J+1) + 3J^2(J+1)^2$
$O_6^0 = 231J_z^6 - 315J(J+1)J_z^4 + 735J_z^4 + 105J^2(J+1)^2 J_z^2 -$ $-525J(J+1)J_z^2 + 294J_z^2 - 5J^3(J+1)^3 + 40J^2(J+1)^2 - 60J(J+1)$
$O_4^4 = \frac{1}{2}(J_+^4 + J_-^4)$
$O_6^4 = \frac{1}{2}\{(11J_z^2 - J(J+1) - 38)(J_+^4 + J_-^4)\}_S$
$O_6^6 = \frac{1}{2}(J_+^6 + J_-^6)$

Summing the abovementioned we can write the crystal field potential in the following form:

$$V = \sum_{k=2,4,6} \sum_q a_k A_k^q \langle r^k \rangle O_k^q = \sum_k \sum_q a_k C_k^q O_k^q; \qquad (21)$$

here $\langle r^k \rangle$ – the average value of r^k obtained by averaging on atomic wave functions. In most cases neither the coefficients A_k^q, nor the radial parts of atomic wave

functions are not precisely known; therefore the products $A_k^q\langle r^k\rangle = C_k^q$ can be considered as fitting parameters. They are called a "crystal field parameters" and are found, as a rule, from optical spectra of rare-earth ions in crystals.

The result of effect of potential (21) within a set of states with given J can be illustrated rather simply. The equivalent operators of the type O_4^0 contain only J_z and, hence, have only diagonal matrix elements for $2J+1$ states characterized by various values of the magnetic quantum number J_z or M. These diagonal matrix elements are identical for the states $+J_z$ and $-J_z$ since the operators contain only even degrees of J_z. The states with different $|J_z|$ values have, generally speaking, different energies; therefore the crystal potential containing only operators O_k^0 will lead to occurrence of some doublets of the type $|\pm M|$ and one singlet $|O\rangle$, if J is integer.

The operators O_k^q for which $q \neq 0$ have only the nondiagonal matrix elements and, hence, mix the states with various M, so the resulting wave functions have the form:

$$\sum_M C_M |J, M\rangle, \tag{22}$$

where, of course, $\sum_M C_M^2 = 1$ to satisfy the normalization requirement. In any such combination the consecutive M values differ on quantity q. For example, the presence of equivalent operator O_6^6 in (21) leads to occurrence of states with the wave functions:

$$C_{M+6}|J, M+6\rangle + C_M|J, M\rangle + C_{M-6}|J, M-6\rangle,$$

in which the number of terms does not exceed three, since the maximum value of J in the ground state is equal 8 (Ho^{3+} ion, $4f^{10}$, $^5I_8$).

1.5. Zeeman effect

When the secular equation is solved, i.e. the ion energy levels in a crystal field and the corresponding wave functions are found, it is necessary to evaluate the splitting of these levels by an external magnetic field. We know (see Tables 1.2) that under the effect of a crystal electric field, either doublets and quadruplets (ions with odd number of electrons), or singlets, doublets and triplets (ions with an even number of electrons) do appear. Since the intervals between the energy levels in a crystal field are much larger the Zeeman splitting in usual magnetic fields, the magnetic resonance transitions are observed, as a rule, only between the components of Stark energy levels. The spin-lattice interaction in compounds with rare-earth elements is very strong at room temperature, therefore the experiments should be performed at such low temperatures that only the lowest level is actually populated. It is clear that EPR observation will be possible if this level is not a singlet.

To determine the resonance condition it is necessary to calculate the Zeeman effect for the lowest level. In the first approximation, when only the matrix elements between the states with the given value **J** are considered, the Zeeman operator $\mathsf{H}_Z = \mu_B(\mathbf{L} + 2\mathbf{S})H$ is reduced to the simple from: $\mathsf{H}_Z = g_J \mu_B \mathbf{HJ}$. Thus, calculation of the Zeeman effect of the first order is reduced to finding the matrix elements J_x, J_y, J_z for the lower group of states. Suppose that the doublet is the lowest Stark energy level of a rare-earth ion. Suppose also that the crystal electric field has the axial symmetry (trigonal, tetragonal or hexagonal). Then the matrix elements J_x и J_y

are equal, but differ, generally speaking, from the matrix element J_z, so the Zeeman effect within the lower doublet is described by the spin Hamiltonian with effective spin S=1/2 and anisotropic g-tensor:

$$\mathsf{H}_S = g_{||}\mu_B H_z S_z + g_\perp \mu_B \left(H_x S_x + H_y S_y \right), \tag{23}$$

Here

$$g_{||} = 2g_J \left\langle + \left| J_z \right| + \right\rangle, \; g_\perp = g_J \left\langle + \left| J_+ \right| - \right\rangle, \tag{24}$$

and $\left|+\right\rangle$ and $\left|-\right\rangle$ – two components of a doublet of the type (22). For conservation of exact sign of $g_{||}$ which is important for some purposes, two states $\left|+1/2\right\rangle$ and $\left|-1/2\right\rangle$ of the effective spin shall be chosen so that the identity shall be satisfied:

$$g_\perp \left\langle +1/2 \left| S_+ \right| -1/2 \right\rangle \equiv g_J \left\langle + \left| J_+ \right| - \right\rangle.$$

Physically this identity is required in order that the spin Hamiltonian gave the exact intensities of the resonance transitions caused by the variable magnetic field H_1 with the circular polarization.

In the case of strong magnetic fields when the Zeeman energy is not so small in comparison with the splittings in a crystal field, it can appear that it is necessary to consider the higher order effects, not only the first one. The Zeeman effect of the second order leads to that both sublevels of a doublet are shifted on the same value, proportional to H^2; this does not change the frequency of transition between the doublet states. The Zeeman effect of the third order affects the frequency of transition since it can have different signs for two components of a doublet and shifts them in the opposite directions. This splitting can be considered as a by-effect of the second order Zeeman effect. Really, the latter changes the wave functions of the lower doublet in such a manner that they take the form $\left\{ \left|+\right\rangle + \sigma \left|+'\right\rangle \right\}$ и $\left\{ \left|-\right\rangle + \sigma \left|-'\right\rangle \right\}$. The coefficient σ determines the impurity of the other states and is proportional to the field H. If now we calculate the Zeeman splitting of the first order, using the new states, then, besides the main term proportional to H, we will obtain the correction to the energy, proportional to $H\sigma^2$, i.e. H^3. This

effect has the greatest value for the doublets which do not split in the magnetic field perpendicular to the axis *c* in the first approximation ($g_\perp$=0), but may split in the third order and give a weakly allowed transition in the strong magnetic fields.

1.6. Magnetic hyperfine interaction

Let's consider the interaction of the nuclear magnetic moment with the local magnetic field created by environmental electrons. This field is caused partly by the orbital motion of electrons and partly by their spin magnetism. For the free ion in the case of *LS*-coupling the resulting field created by electrons quickly precesses around a vector of the total moment of momentum **J**. With close approximation it is possible to restrict the consideration of only the field component which is parallel to **J** and, hence, is conserved at motion. It gives the possibility to reduce the magnetic hyperfine interaction Hamiltonian to the simple form:

$$\mathsf{H}_{HF} = A_J \mathbf{JI}. \tag{25}$$

The operator of the magnetic interaction of a nucleus with electrons is generally has the following form:

$$\mathsf{H}_{HF} = \gamma \mathsf{h} I \cdot 2\mu_B \sum_i \left\{ \frac{\mathbf{l}_i}{r_i^3} - \frac{\mathbf{s}_i}{r_i^3} + \frac{3(\mathbf{s}_i \mathbf{r}_i)\mathbf{r}_i}{r_i^5} + \frac{8\pi}{3} \mathbf{s}_i \delta(\mathbf{r}_i) \right\}. \tag{26}$$

The main electronic configuration of the paramagnetic ion does not contain the unpaired S-electrons, therefore the last term in curly brackets (26) usually does not contribute to the hyperfine interaction constant of the free ion A_J in (25). If the ground term of a paramagnetic ion has at least slight "impurity" of the excited configurations containing unpaired S-electrons (they are called s-configurations) then the contribution of the contact interaction in A_J becomes different from zero. As experience shows, in case of the rare-earth atoms the contact contribution to the

hyperfine interaction is insignificant, therefore we can neglect it. Then for the hyperfine interaction constant we have:

$$A_J = 2\mu_B \gamma \hbar \left\langle r^{-3} \right\rangle \left\langle J \left\| N \right\| J \right\rangle; \tag{27}$$

here γ - gyromagnetic ratio of nucleus of a rare-earth ion, $\left\langle J \left\| N \right\| J \right\rangle$ – coefficient which value can be found in Tables (see [1, 2]).

Within the approach that takes into account only the matrix elements between the states with given *J*, the calculation of the magnetic hyperfine interaction is very simple, since, as well as for the Zeeman effect calculation, only the matrix elements of the operator *J* are required here. Hence, there is the linear relation between the hyperfine and Zeeman interactions. For some subspace with (2*J*+1) states which can be represented by fictitious spin **S** and for which the Zeeman interaction has the form $\mu_B \mathbf{H} \cdot \hat{g} \mathbf{S}$, the hyperfine interaction will look like $\mathbf{S} \cdot \hat{A} \mathbf{I}$, where $\hat{A}$ – a tensor which, obviously, has the same main axes, as the *g*-tensor. The principal values of these tensors are related by a relationship:

$$\frac{A_x}{g_x} = \frac{A_y}{g_y} = \frac{A_z}{g_z} = \frac{A_J}{g_J}. \tag{28}$$

This relationship means that at measurements with fixed frequency in a changing magnetic field the hyperfine splittings in EPR spectra will be identical for field directions along each of the main axes. In the presence of anisotropy for any field directions this relationship will be invalid because of difference of transformation properties of $\hat{g}$ and $\hat{A}$ (see [2], chapter 3):

$$g^2 = l^2 g_x^2 + m^2 g_y^2 + n^2 g_z^2, \tag{29}$$

$$g^2 A^2 = l^2 g_x^2 A_x^2 + m^2 g_y^2 A_y^2 + n^2 g_z^2 A_z^2; \tag{30}$$

here *l*, *m*, *n* – direction cosines of the field **H** relative the main axes of the *g*-tensor. From (28) it follows also that we can, without data on the crystal field, find the value of A_J only from the magnetic resonance experiments using the experimental values of $\hat{g}$ and $\hat{A}$ along the main axes.

Table 1.5

Atomic number	Ion	Isotope	Abundance, %	Nuclear spin I	A_J/h, MHz
59	Pr^{3+}	141	100	5/2	+1093 (10)
60	Nd^{3+}	143	12.3	7/2	-220.3 (2)
		145	8.3	7/2	-136.9 (1)
61	Pm^{3+}	147	radioactive	7/2	(+) 599 (6)
62	Sm^{3+}	147	15.0	7/2	-240 (3)
		149	13.9	7/2	-194 (3)
65	Tb^{3+}	159	100	3/2	+530 (5)
66	Dy^{3+}	161	19.0	5/2	-109.5 (22)
		163	24.9	5/2	+152.4 (30)
67	Ho^{3+}	165	100	7/2	+812.1 (10)
68	Er^{3+}	167	22.9	7/2	-125.3 (12)
69	Tm^{3+}	169	100	1/2	(–) 393.5
70	Yb^{3+}	171	14.4	1/2	+887.2 (15)
		173	16.2	5/2	-243.3 (4)

These simple results lapse when the crystal field mixes the states with different *J*. The reason is that though the matrix elements of the hyperfine interaction operator can be always bound with the matrix elements of the Zeeman operator, the constants of proportionality for these two operators change unequally. Thus, practically one appraises about applicability of the approach, in which *J*-mixing is neglected, to what extent the relation (28) is satisfied.

Table 1.5 shows the values of the magnetic hyperfine interaction constants A_J for free trivalent ions found from the EPR spectra in the ionic crystals.

2. Examples of EPR spectra calculations of rare-earth ions in ionic crystals

2.1. The Nd^{3+} ion in neodymium ethylsulfate

Let's perform a calculation of EPR spectrum of the Nd^{3+} ions in ethylsulfate at the liquid helium temperature. The crystal field in ethylsulfates has a C_{3h} symmetry and is described by the Hamiltonian

$$V = \alpha C_2^0 O_2^0 + \beta C_4^0 O_4^0 + \gamma C_6^0 O_6^0 + \gamma C_6^6 O_6^6. \qquad (31)$$

The values of the crystal field parameters have been found from the optical spectra of the Nd^{3+} ions in $La_{1-x}Nd_x(C_2H_5SO_4)_3 \cdot 9H_2O$ crystals:

$$C_2^0 = 58.2\text{cm}^{-1},\ C_4^0 = -68.2\text{cm}^{-1},\ C_6^0 = -42.7\text{cm}^{-1},\ C_6^6 = 595\text{cm}^{-1}.$$

The Stevens coefficients are known from tables (see [1,2]):

$$\alpha = -\frac{7}{3^2 \cdot 11^2},\ \beta = -\frac{2^3 \cdot 17}{3^3 \cdot 11^3 \cdot 13},\ \gamma = -\frac{5 \cdot 17 \cdot 19}{3^3 \cdot 7 \cdot 11^3 \cdot 13^2}.$$

To calculate the splitting by the crystal field of the ground level $^4I_{9/2}$ of the Nd^{3+} ion (J=9/2) it is necessary to calculate the matrix elements of the operator (31) by means of wave functions $\left|J = 9/2,\ M\right\rangle$, where M = 9/2 7/2, …,–9/2. The diagonal matrix elements $\left\langle M\left|V\right|M\right\rangle$ and elements of the type $\left\langle M\left|V\right|M \pm 6\right\rangle$ will be different from zero. Using the tables of matrix elements of equivalent operators in [1, 2] we write a perturbation matrix (in cm^{-1}) (Table 2.1). The secular equation can be easily solved since the matrix partitions into submatrices of the first and second orders.

Table 2.1

M	9/2	7/2	5/2	3/2	1/2	–1/2	–3/2	–5/2	–7/2	–9/2
9/2	41.0						–74.6			
7/2		–131.1						–113.9		
5/2			55.6						–113.9	
3/2				60.8						–74.6
1/2					–26.4					
–1/2						–26.4				
–3/2	–74.6						60.8			
–5/2		–113.9						55.6		
–7/2			–113.9						–131.1	
–9/2				–74.6						41.0

Table 2.2

M	±7/2	m5/2
±7/2	–131.1	–113.9
m5/2	–113.9	55.65

All levels appear to be doubly degenerate (Kramers doublets), their energy is equal to –185,–26,–23, 108 and 126 cm^{-1}, respectively. The lower level energy E =–185 cm^{-1} is obtained from the two submatrices (see Table 2.2). It is evident from the table that the lower level is a doublet:

$$|\pm\rangle = C_{\pm 7/2}\left|\pm 7/2\right\rangle + C_{\mp 5/2}\left|\mp 5/2\right\rangle.$$

The coefficients in the wave functions are found from the normalization requirement $\left(C_{\pm 7/2}\right)^2 + \left(C_{\mp 5/2}\right)^2 = 1$ and the equation is $\left(-131.1 - E\right)C_{\pm 7/2} - C_{\mp 5/2}\cdot 113.9 = 0$ in which we put E =–185 (cm^{-1}). As a result we obtain the wave functions of the lower doublet:

$$|\pm\rangle = 0.905\left|\pm 7/2\right\rangle + 0.431\left|\mp 5/2\right\rangle.$$

The Lande factor of the free Nd^{3+} ion is g_J = 8/11, therefore for the *g*-tensor components (24) we find:

$$g_{||} = 2g_J\left\langle +\left|J_z\right|+\right\rangle = 3{,}48,$$

$$g_{\perp} = g_J\left\langle +\left|J_+\right|-\right\rangle = 2{,}27.$$

The agreement with the experimental values $g_{||} = 3.535$ and $g_{\perp} = 2.072$ can be improved if we consider an impurity of excited states $^4I_{11/2}$ for the calculation of the perturbation matrix.

It is necessary to bear in mind that EPR observation on Kramers doublet is not always possible. For example take the topmost doublet with the energy of 126 cm^{-1}; the following wave functions correspond to it:

$$|\pm\rangle = 0.655\left|\pm 9/2\right\rangle + 0.756\left|\mp 3/2\right\rangle.$$

Unlike functions $|+\rangle$ and $|-\rangle$ of the conjugated Kramers states ΔM = 9/2 – 3/2 >1 and consequently $g_{\perp}$ = 0. If we direct a static magnetic field along the *c* axis of the crystal ($\mathbf{H} \| z$) then the EPR effect will be absent, because the probability of a magnetic dipole transition between the Zeeman sublevels is equal to zero (irrespective of the magnetic field direction). If the magnetic field is perpendicular to the *c* axis of crystal then there is no Zeeman splitting.

2.2. The Ce^{3+} ion in the crystal field with cubic symmetry

The field with cubic symmetry is described by the Hamiltonian

$$V = \beta C_4^0 \left(O_4^0 + 5O_4^4 \right) + \gamma C_6^0 \left(O_6^0 - 21O_6^6 \right) \tag{32}$$

For the Ce^{3+} ion in the ground state $J = 5/2$, therefore it is possible to set $\gamma = 0$ in (32). According to Table 1.2 the sixfold degenerate level $^2F_{5/2}$ of the free ion is split on one doublet and one quadruplet. The perturbation matrix is given in Table 2.3. From it we find the energies and the corresponding wave functions:

$$E_{1,2} = -240\delta C_4^0,\ \Psi_{1,2} = \sqrt{\frac{1}{6}}\left|\pm 5/2\right\rangle - \sqrt{\frac{5}{6}}\left|\mp 3/2\right\rangle;$$

$$E_{3,4,5,6} = 120\delta C_4^0,\ \Psi_{3,4} = \sqrt{\frac{5}{6}}\left|\pm 5/6\right\rangle + \sqrt{\frac{1}{6}}\left|\mp 3/2\right\rangle,$$

$$\Psi_{5,6} = \left|\pm 1/2\right\rangle.$$

For the Ce^{3+} ion the Stevens coefficient is $\beta = \frac{2}{3^2 \cdot 5 \cdot 7} > 0,$ therefore in the case of positive value of the parameter C_4^0 the doublet

$$\left|\pm\right\rangle = \sqrt{\frac{1}{6}}\left|\mp 5/2\right\rangle - \sqrt{\frac{5}{6}}\left|\pm 3/2\right\rangle$$

Table 2.3

M	5/2	3/2	1/2	–1/2	–3/2	–5/2	
5/2	1				$\sqrt{5}$		
3/2		–3				$\sqrt{5}$	
1/2			2				$\times 60\beta C_4^0$
–1/2				2			
–3/2	$\sqrt{5}$				–3		
–5/2		$\sqrt{5}$				1	

is the lowest Stark level with the isotropic g-tensor:

$$g = \frac{10}{6} \cdot g_J = \frac{10}{7}.$$

3. Problem

1. Compose an energy matrix of the Yb^{3+} ion ($^2F_{7/2}$) in the crystal electric field of cubic symmetry. Find the energy levels and the wave functions of the Yb^{3+} ion. Calculate the *g*-factors of the doublets Γ_6 (±7/2, μ1/2) and Γ_7 (±5/2, μ3/2)

Instructions. 1) The Hamiltonian shall be presented in the form

$$\mathsf{H}_{KP} = \beta C_4^0 \left(O_4^0 + 5O_4^4 \right) + \gamma C_6^0 \left(O_6^0 - 21O_6^4 \right);$$

here β, γ – Stevens coefficients,

C_4^0, C_6^0 – crystal field parameters,

O_4^0, O_4^4, O_6^0, O_6^4 – equivalent operators.

2) Subdivide the 8th order matrix into four 2nd order matrices.

3) Write the matrix elements using the common factors *F*(4) and *F*(6);

For example, $\left\langle \pm 7/2 \left| \mathsf{H}_{KP} \right| \mp 1/2 \right\rangle =$

$$= \beta C_4^0 \cdot 5 \left\langle \pm 7/2 \left| O_4^4 \right| \mp 1/2 \right\rangle - \gamma C_6^0 \cdot 21 \left\langle \pm 7/2 \left| O_6^4 \right| \mp 1/2 \right\rangle =$$

$$= \beta C_4^0 \cdot F(4) \sqrt{35} - \gamma C_6^0 \cdot F(6) 3\sqrt{35}.$$

4) At diagonalization of matrices separate the matrix elements on $\gamma C_6^0 F(6)$ and use the abbreviation

$$\beta C_4^0 F(4) / \gamma C_6^0 F(6) = \rho;$$

For example, $\left\langle \pm 7/2 \left| \mathsf{H}_{KP} \right| \mp 1/2 \right\rangle \Rightarrow \sqrt{35}\rho - 3\sqrt{35}.$

5) Use the crystal field parameters for energy calculation of the electronic states

$$C_4^0 = -240\text{см}^{-1},\ C_6^0 = 41{,}8\text{см}^{-1};$$
$$\beta = -1{,}7316\cdot 10^{-3},\ \gamma = 1{,}48\cdot 10^{-4},$$
$$F(4) = 60,\ F(6) = 1260.$$

6) Calculate the *g*-factors of the doublets Γ_6, Γ_7 from the equation

$$g(\Gamma_j) = 2g_J \cdot \left|\left\langle \Gamma_j \left| J_z \right| \Gamma_j \right\rangle\right|.$$

2. Calculate the parameters of the spin Hamiltonian (S = 1/2) of the ground electronic doublet of the Yb^{3+} ion in the cubic crystal field of PbF_2:

$$\mathsf{H}_S = g\mu_B \mathbf{HS} + A\mathbf{SI}.$$

Calculate the energies of the electron-nuclear states and construct the energy level diagrams for even and odd isotopes (see Table 3.1).

Table 3.1

Isotope	Natural abundance, %	Nuclear spin, I
^{168}Yb	0.1	0
^{170}Yb	3.2	0
^{172}Yb	21.9	0
^{174}Yb	31.6	0
^{176}Yb	12.6	0
^{171}Yb	14.4	1/2
^{173}Yb	16.2	5/2

Calculate the resonance fields of extreme lines in the EPR spectra of both odd isotopes.

Instructions. 1) Consider the field **H** applied along the axis *z* and use the simplified form of the spin Hamiltonian:

$$\mathsf{H}_S = hS_z + AS_zI_z + \frac{1}{2}A\left(S_+I_- + S_-I_+\right)$$

($h = g\mu_B H$).

2) At evaluation of the parameters ^{171}A and ^{173}A use the following values of the hyperfine interaction constants:

$$^{171}A_J/h = 887.2 \text{ MHz}, \; ^{173}A_J/h = -243.3 \text{ MHz}.$$

3) Reduce the energy matrices of the electron-nuclear states (4th order for ^{171}Yb and 12th order for ^{173}Yb) to 2nd order matrices.

4) Prove the validity of the relations:

$$\left|^{171}A\right| = 2g\mu_B \frac{H_0^2}{^{171}\Delta}\left[\left(1+\frac{^{171}\Delta^2}{H_0^2}\right)^{1/2}-1\right],$$

$$\left|^{173}A\right| = 10g\mu_B \frac{H_0^2}{^{173}\Delta}\left[\left(1+\frac{^{173}\Delta^2}{25H_0^2}\right)^{1/2}-1\right];$$

here g – factor of spectroscopic splitting of the ground doublet of the Yb^{3+} ion, H_0 – resonance field of even ytterbium isotopes (in Oersteds), $^{171}\Delta$ and $^{173}\Delta$ – intervals between the extreme lines of EPR spectra of odd ytterbium isotopes (in Oersteds).

3. Perform recording of the EPR spectrum of the Yb^{3+} ions in PbF_2 crystal at temperature 4.2 K. Measure the resonance fields and identify the spectral lines. Find the parameters of the spin Hamiltonian (g, ^{171}A, ^{173}A) from the EPR spectrum and compare these with calculations (take the g-factor of the free DPPH radical equal to 2.0057).